

# POLITECNICO DI TORINO

Corso di Laurea Magistrale

in Ingegneria per l'Ambiente e il Territorio

---

Tesi di Laurea Magistrale

## RECONNECTION OF AN AQUIFER PARTITIONED BY A RAILWAY TUNNEL



**Studente**

Alice Ancora

**Relatori**

Prof. Giovanni De Cesare  
Prof. Costantino Manes

---

Anno Accademico 2018/2019



---

## Acknowledgements

I would like to express my gratitude to Politecnico di Torino, where I performed my academic studies, which gave me the opportunity to spend the last year of my Master abroad.

All my thankfulness to École Polytechnique Fédérale de Lausanne (EPFL), that welcomed me like exchange student, giving me the possibility to get in touch with this cosmopolitan reality, and allowing me to increase and improve my technical knowledges. In particular, thank to the Laboratory of Hydraulic Construction (LCH), where I worked for my Master thesis, which hosted me for six months and gave me continuous support and the opportunity to meet very nice people.

Finally, all my gratitude to my parents that allowed me to study far away from my hometown, to Giuseppe for his continuous support, and to all the people that I met during this journey, sharing good as well as hard moments, but making this experience unforgettable!

Thank you! Merci beaucoup! Grazie!

---

---

## Abstract

*The objective of this study was to assess the performance and efficiency of an innovative groundwater transfer system built with the purpose of reconnecting an unconfined aquifer broken off by the construction of a railway covered trench.*

*A rise of the groundwater table can be, in certain circumstances, a significant hazard for the structures in an urban environment. The level of the aquifer may rise for different reasons, one example is due the construction of a tunnel at shallow depth below the piezometric surface which provokes the obstruction of the groundwater flow in a direction perpendicular to the tunnel axis. Instead of using a traditional pumping device, the prototype of the groundwater transfer system involved in this study is a self-priming free-surface siphon, developed at the Laboratory of Hydraulic Construction (LCH) at École Polytechnique Fédérale de Lausanne (EPFL) in 2017. Siphons were built in field in June 2018 and are currently in a monitoring phase. Measurements of groundwater levels into wells are constantly recorded.*

*The first part of this study was focused on the understanding of the main principles of the siphon system and on the hydrogeological context in which is located. Siphons work thanks to a specialized vortex chamber installed in a variable pressure “sealed box”, located at the end of the horizontal pipe of the siphon. With a multi-phase flow condition of both water and air, water is conveyed with air in the downstream pipe, maintaining the system stall-free.*

*In the second part, the aim was to evaluate if the groundwater transfer system is working as it was defined during the design phase, and to quantify its effect on the aquifer. Firstly, the discharge in siphons system was assessed with Darcy-Weisbach approach and compared with the one adopted in the design phase. The study was focused on siphons n.18, 19, and 20, i.e. the ones with a better connection.*

*Afterwards, the efficiency of the artificial drainage trench built along the system was assessed: the response was conducted by considering the estimated flow rate and water levels registered by automatic piezometers in siphons. By means of theory of pumping tests, lowering in the upstream part and rises in the downstream part were assessed.*

*In order to have a global understanding of the process, a response of the real aquifer was conducted, in the upstream as well as in the downstream sector of the siphons system, at different distances from the drainage trench. A simplified system was adopted, by considering a uniform, homogeneous, and constant aquifer.*

*The obtained results show that, in almost 8 months of operating system, aquifer has a satisfactory reaction: a decrease in difference of water levels ( $\Delta H$ ) of approximately 0.80 meters*

---

*was registered in the wells, by around 0.60 meters along the drainage trench, and by around 0.50 meters in the aquifer at a distance of 50 meters from the drainage trench.*

*To assess more efficiently the flow rate in the system, on 29<sup>th</sup> July a flow meter was installed in field on siphon n.19. When first data will be available, it will be possible to compare these values with ones obtained in an analytical approach, and also to compute more detailed studies on the relationship between discharge and water levels in the three siphons.*



---

# Table of Contents

<b>Abstract</b> .....	I
<b>Notations</b> .....	VI
<b>Chapter 1. Introduction</b> .....	1
1.1 <i>Objectives and Methodology</i> .....	1
1.2 <i>Effects of rising groundwater levels</i> .....	1
1.3 <i>CEVA railway project and its effect on the aquifer</i> .....	2
1.4 <i>Proposed alternatives to reconnect the aquifer</i> .....	3
<b>Chapter 2. Self-priming Free-surface siphon</b> .....	6
2.1 <i>Siphon principles</i> .....	6
2.2 <i>Siphon for CEVA project</i> .....	7
2.2.1 <i>Physical Model</i> .....	7
2.2.2 <i>Parametric studies on vortex chamber</i> .....	10
<b>Chapter 3. Geological and hydrogeological overview</b> .....	14
3.1 <i>General context</i> .....	14
3.2 <i>Local context</i> .....	14
3.3 <i>Pumping and infiltration tests</i> .....	18
3.4 <i>Current situation</i> .....	18
<b>Chapter 4. Study of the discharge</b> .....	21
4.1 <i>Estimation of water level-discharge relationship on the prototype</i> .....	21
4.2 <i>Discharge estimation on the siphons in situ</i> .....	24
4.2.1 <i>Results</i> .....	24
4.3 <i>Estimation of fitting and local head losses</i> .....	26
<b>Chapter 5. Analytical study of the drainage trench</b> .....	28
5.1 <i>Analytical solutions of differential flow equation</i> .....	28
5.2 <i>Estimation of groundwater levels evolution</i> .....	32
5.3 <i>Results and Discussion</i> .....	35
<b>Chapter 6. Analytical study of the aquifer</b> .....	38
6.1 <i>Differences between drainage trench and aquifer</i> .....	38
6.2 <i>Estimation of groundwater levels evolution</i> .....	38
6.3 <i>Results and Discussion</i> .....	40
<b>Chapter 7. Conclusions</b> .....	44
7.1 <i>Final discussion</i> .....	44
7.2 <i>Future work</i> .....	48
<b>Appendix A – Additional equations</b> .....	52
<b>Appendix B – Discharge during first pumping test</b> .....	54
<b>Appendix C – Estimation of groundwater levels evolution in drainage trench</b> .....	55
<b>Appendix D - Estimation of groundwater levels evolution in the aquifer</b> .....	57
<b>References</b> .....	60



---

## Notations

$F_i$ : inlet Froude number  $F_i = Q/\sqrt{g}b^{3/2}h$

Q: discharge [m<sup>3</sup>/s]

$\Delta H$ : difference of water level between upstream and downstream [m]

h: water level [masl]

r: distance from a given well [m]

s(r,t): groundwater lowering [m]

T: transmissivity [m<sup>2</sup>/s]

$S_y$ : specific yield [-]

S: storage coefficient [-]



---

# Chapter 1. Introduction

## 1.1 *Objectives and Methodology*

The objective of this study is to assess the efficiency of an innovative groundwater transfer system built with the purpose of reconnecting an unconfined aquifer divided by the construction of a railway covered trench. The railway tunnel blocked the groundwater flow, which its direction was mainly perpendicular to the tunnel axis, and it partitioned the aquifer into an upstream and downstream sector.

Self-priming multiphase siphons were designed at Laboratory of Hydraulic Construction at EPFL, Lausanne, in 2017 and since 2018 they are in situ, built over the railway tunnel with the addition of a drainage trench. The system is currently in operation and on-site measurements of groundwater levels are available.

The main goal is to quantify the effect of the siphons on the aquifer, verifying if the groundwater transfer system functions as it was predicted in the design phase. To achieve the objective, the main working principles of siphons will be studied and data from piezometers, and pumping tests will be analyzed.

In particular, in this first chapter the main factors linked with the alteration of a groundwater levels are briefly presented, as well as the reasons that provoked the division of that particular shallow aquifer. The three main proposed solutions for its reconnection are discussed.

Chapter 2 is focused on the understanding of the principles at the base of self-priming free-surface siphon and on the parametric studies conducted on it.

Chapter 3 deals with the main hydrogeological characteristics of the site and on the available studies (e.g. pumping tests) conducted so far.

In Chapter 4, an estimation of the discharge in the siphons in situ is assessed and discussed. These assessments are carried out on the basis of the experiments conducted on the physical model and they are focused on siphon n.18, 19, and 20, i.e. the ones with a better connection. The effects of the siphons system on the aquifer is quantified. Firstly, the artificial longitudinal drainage trench built along the siphons is considered (Chapter 5). Afterwards, the effects in the real aquifer is assessed, considering three different distances from the drainage trench (Chapter 6).

Finally, the effects of siphons operation on the aquifer are discussed in Chapter 7 and future strategies are proposed.

## 1.2 *Effects of rising groundwater levels*

A modification of the groundwater table can be, in certain circumstances, a significant hazard for the urban environment. Even in rural areas, a rising of groundwater levels can adversely affect the root system of the vegetation and therefore influence the local ecosystem. In addition to well-known factors that provoke the alteration of groundwater levels (such as the seasonal discharge and recharge of shallow free aquifers), one other cause could be the construction of a long tunnel at shallow depth below the piezometric surface if that structure creates an obstruction of the groundwater flow in a direction perpendicular to the tunnel axis [1].

The presence of an underground structure can have an impact on the flow of the groundwater

in mainly two different ways. It could act as obstacle to the flow affecting the hydrodynamic parameters of the aquifer and it could also influence the mass balance of the flow system [2]. In particular, the presence of a tunnel forces the groundwater to evade it by locally increasing the length of the flow path and consequently the corresponding flow velocity. The extra energy loss that is required is provided by the locally increased hydraulic gradient in the “ray of influence”. In turn, the hydraulic gradient causes a moderate rise of the water table in the upstream part. This effect decreases when the distance from the tunnel increases [1]. However, if groundwater table can rise reaching the surface, flooding risk may occur.

According to Marinou & Kavvas [1], the magnitude of the increase of water table depends on the size of the tunnel, on its depth below the original water table and on the hydraulic gradient in the direction normal to the tunnel axis. The time required to reach the steady-state condition depends on the hydraulic characteristics of the aquifer as well as the geometrical characteristics of the structure. For values of hydraulic gradient around 0.5-5%, the groundwater level rise of the order of 1-10% of the tunnel height for submerged tunnel located just below of the original water table.

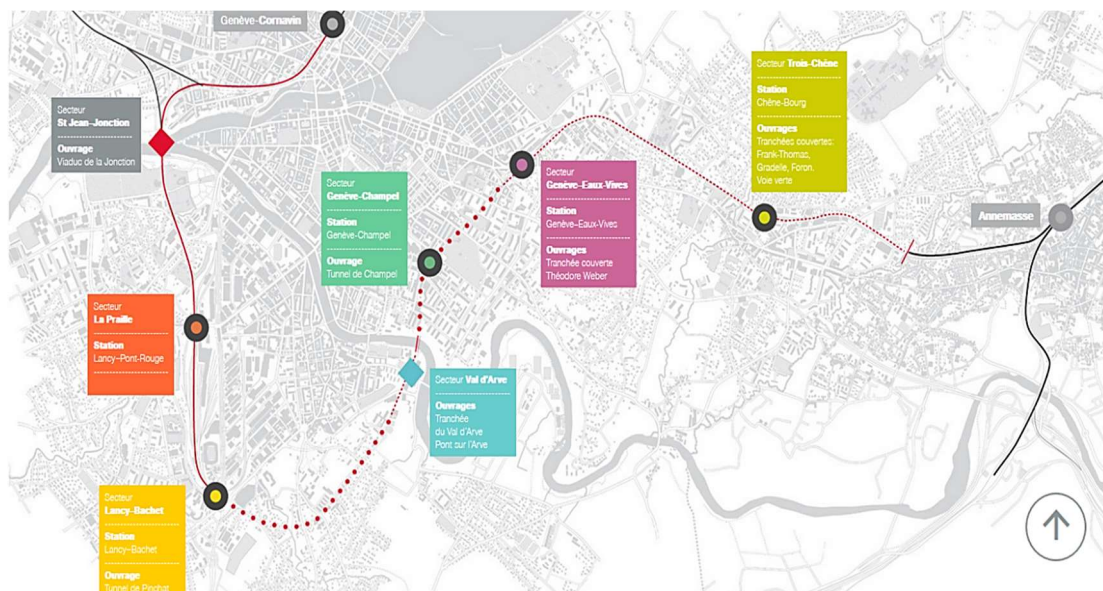


Figure 1 Representation of CEVA railway link and its seven stations. (Source [3])

### 1.3 CEVA railway project and its effect on the aquifer

The railway tunnel involved in this study is part of a big project called CEVA (Cornavin-Eaux-Vives-Annemasse). It is a 16 km long railway line, designed to connect the Geneva Cornavin main station with the French city of Annemasse, passing through Eaux-Vives main station (Figure 1). The main part of the link is in the Swiss area, the last 2 kilometers are in France. This is a strategic project that, when completed at the end of 2019, will link more than 230 km of tracks between Switzerland and France, allowing to create a Regional Express Network (RER) [3].

CEVA will pass through seven train stations which many of them are in important urban agglomerations. For this reason, it will mainly run inside double track line tunnels.

The last railway part, between the Eaux-Vives train station and the Swiss-French border, at beginning organized on surface, it was decided to be buried by creating a covered trench gallery. The decision was taken for the comfort of the residents and in order to avoid increasing the

---

“cut” created by the railway in the Commune of Trois-Chêne (Switzerland). The space left free was redeveloped in a clean site, forming a green cord from Eaux-Vives (Switzerland) to Ambilly (France) [4].

The installation of the covered trench gallery, in this last section, is composed of the Foron river alluvial deposits and resulted in a cut-off of the groundwater, “effect barrage”, partitioning its aquifer into an upstream part (where water levels increased) and downstream part (where water levels decreased), despite of a partial evacuation of water by Foron river. This phenomenon cannot be neglected, due to the significant impact on the safety of the civil engineering structures as well as on the equilibrium of the aquifer.

#### *1.4 Proposed alternatives to reconnect the aquifer*

In order to restore the equilibrium of the groundwater levels on both sides of the tunnel, three main alternatives were proposed: a drainage system, a pumping system, a self-priming siphon system.

The first one was a simple gravitative system that nevertheless presented high costs for the realization and some constraints, due to the presence of the horizontal pipe that would have conveyed the water under the tracks, with high interference risk with the covered trench (Figure 2). Moreover, in this variant the horizontal pipe passed through the impervious layer, and it could have provoked an increasing of the thrust against the covered trench [5].

The second solution was based on the installation of pumps (centrifugal or propeller) controlled by level sondes located in the aspiration and restitution conduits (Figure 3). However, the requested energy for the withdraw was considerable, with an absorbed power estimated to be of the order of 3.3 kW per pump [6]. Since at the beginning the plan was to build 30 wells (30 upstream and 30 downstream) and therefore 30 pumps working concurrently would have been needed, the inconvenient for this solution would have been a very high maintenance cost.

The last hypothesis, a siphon system with self-priming device, represented the most innovative proposal: it doesn't require continuous pumping and energy requirements (Figure 4). However, to work well, it's necessary that the upstream and downstream conduits have a permanent depression.

Instead of using priming pumps, the operating principles of the system is based on the maintenance of a free-surface vortex in a vacuum in what is called “sealed box” which functions by keeping the siphon primed and allowing, in this way, to convey water, with the air, on the other side of the gallery. The purpose of the air-water flow conditions provided by the vortex is to render the system stall-free in the presence of air bubbles, generated by the decrease of the pressure in the horizontal pipe, and also of air entrainment through faulty or damaged pipe work under future working conditions.

In this way, the air is conveyed in downstream tube, allowing not to lose the priming of the siphon. [6]

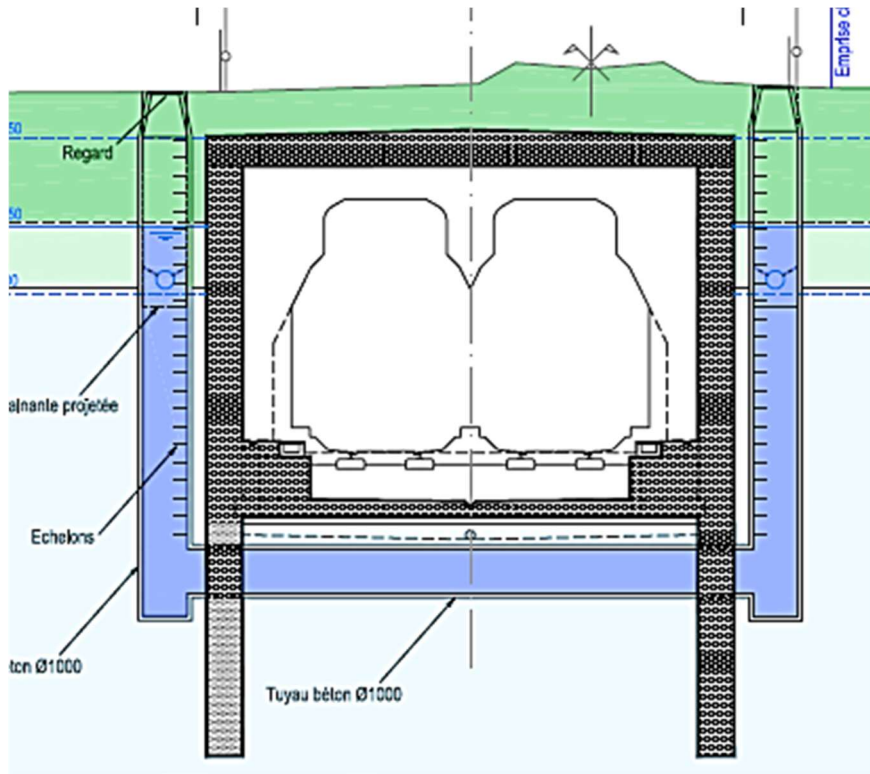


Figure 2 First proposal: drainage system (Source [5])

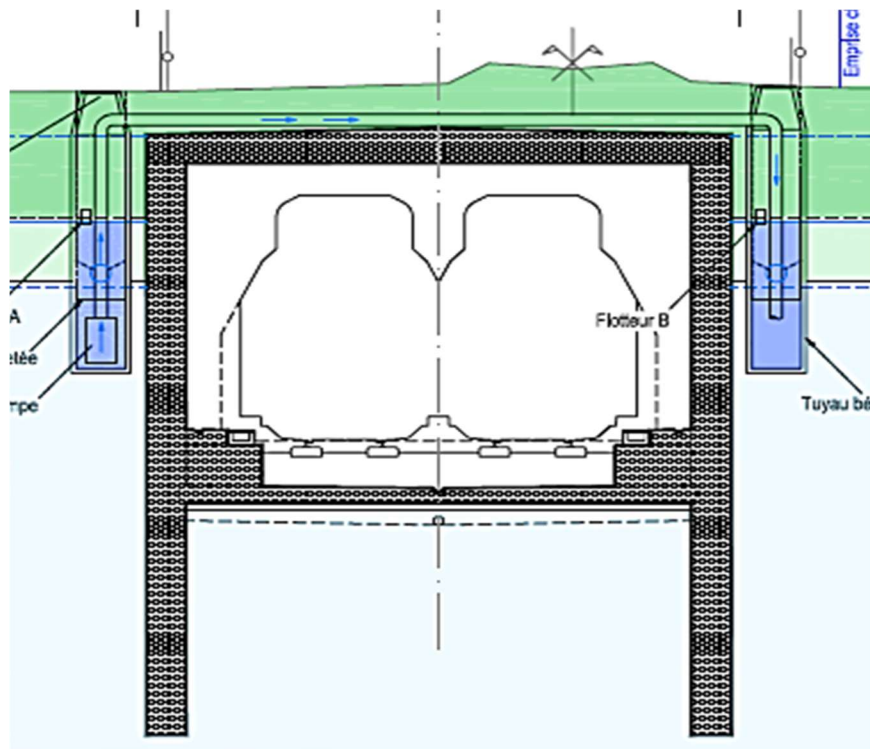
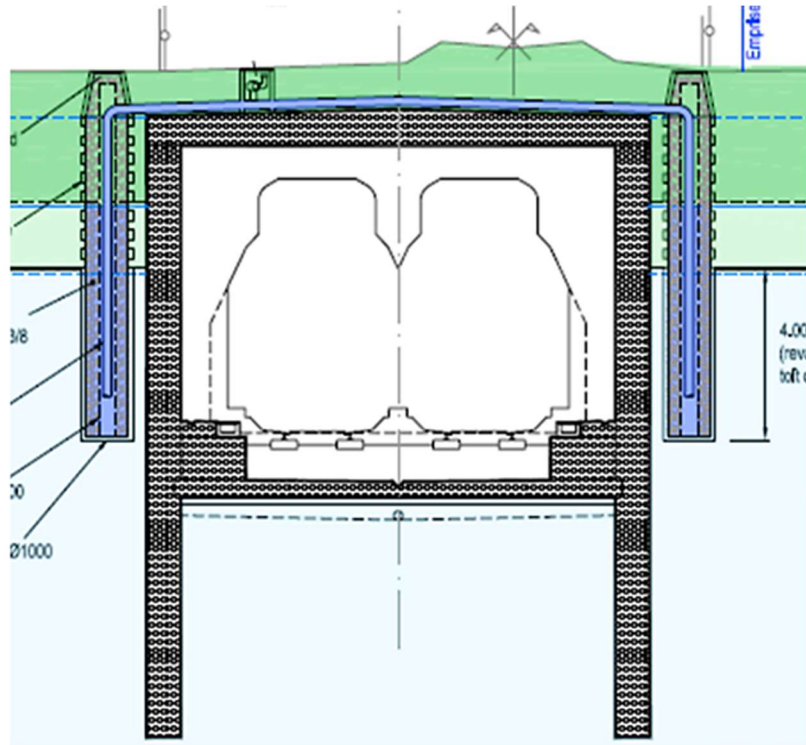


Figure 3 Second proposal: pumping system (Source [5])



*Figure 4 Third proposal: Siphon system (Source [5])*



---

## 2.2 Siphon for CEVA project

The proposed inverse siphon for CEVA project is based on a multiphase flow condition of both water and air. The purpose was to render the system stall-free with the accumulation of air, due to the presence of the horizontal pipe with negative pressures, and also in presence of air entrainment through faulty or damaged pipework [10]. This innovative approach to siphoning, that doesn't require energy if compared to a classical priming pumping system, works thanks to a specialized vortex chamber installed in a variable pressure "sealed box" and located at the end of the horizontal section of the siphon.

A system with similar properties was built in Bern for the water adduction system and it's in service without interruption since 1946. Similarly to the siphons for CEVA project, it doesn't require pumping and it withdraws water from Aar river, that flows in the city and it's characterized by high water quality, without requiring treatments [11]. No other similar studies are available, apart from works about strong vortex flows in the field of drop shafts. These systems were introduced by C. Drioli (1947) as an overflow structure for dams for energy dissipation, and nowadays are also widely used in sewer systems to connect sewers characterized by large elevation gaps [12].

Due to the novelty of the system, a full-scale (1:1) physical model was designed and constructed at the Laboratory of hydraulic constructions at École Polytechnique Fédérale de Lausanne in 2017.

### 2.2.1 Physical Model

The model was constructed at full scale except for the horizontal conduit. For this reason, a spherical valve was used to simulate the range of head losses expected in the full-length pipe.

*Table 1 Main sizes of the model*

Height of the model	6.40 m
Length of the horizontal pipe	4.50 m instead of 15 m of the prototype
Diameter $\phi$	90 mm

As it is showed in Figure 6 and Figure 7, the main parts and instrumentations of the facility built in laboratory are described [10]:

- Circular reservoirs: Supplied by a pump, they simulated the upstream and downstream groundwater levels in real conditions.
- Suspended mobile buckets: They regulated the groundwater levels. They were designed using multiphase model in Flow3D for a maximum discharge of 9 l/s. In order to generate a close circuit, a pump used to supply water to the system and the outlets of the buckets were connected to a main tank.
- Main tank: Its purpose was to pump the water to both reservoirs through a horizontal pipe.
- Butterfly valves: They were installed in the low part, upstream of the reservoirs, to regulate discharge going to each reservoir.
- Pipe in the reservoirs: it has a diameter of 90 mm and conveys the water to the horizontal pipe and therefore to the main siphon components.

- Spherical valve: Located in the up part, it was used to simulate the range of head losses expected in the full-length pipe.

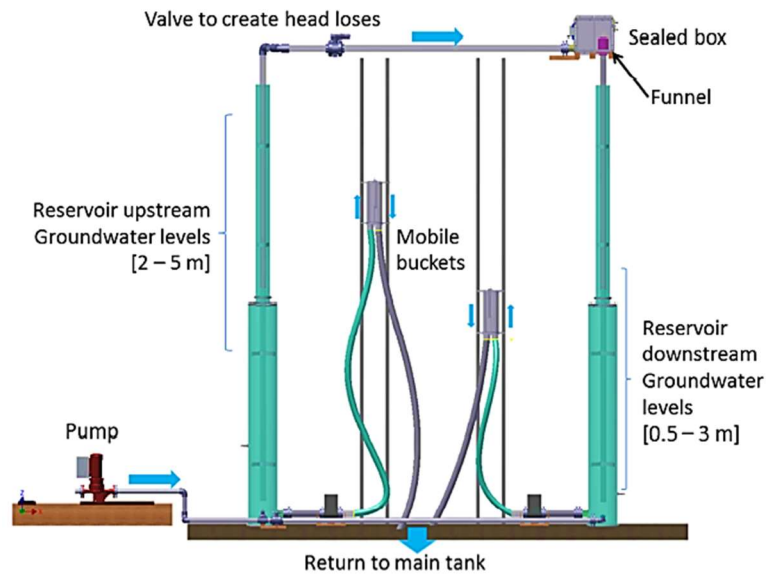


**Figure 6** Schematic representation of the model built in 1:1 scale at LCH (Source [10])

- Sealed box: it's the core of the siphon system, located at the end of the horizontal pipe. It contains the vortex chamber. It is 0,5 m long, 0,5 m wide and 0,4 m high. It was made of 6 Plexiglas plates in order to resist a differential pressure of minus 10 m water column. In the left wall there are two air rotameters (for air discharge measures). In the right wall there is a connection for a vacuum pump, necessary to initiate the siphon.
- Flowmeters: they were placed between the main reservoirs and the mobile buckets, to regulate water discharge
- Pression sensors: they were located upstream and downstream, at 1 and 0,5 m from the bottom of the reservoirs. By knowing the pressure, the water level in the reservoir was also determined in order to assume a hydrostatic pressure distribution.

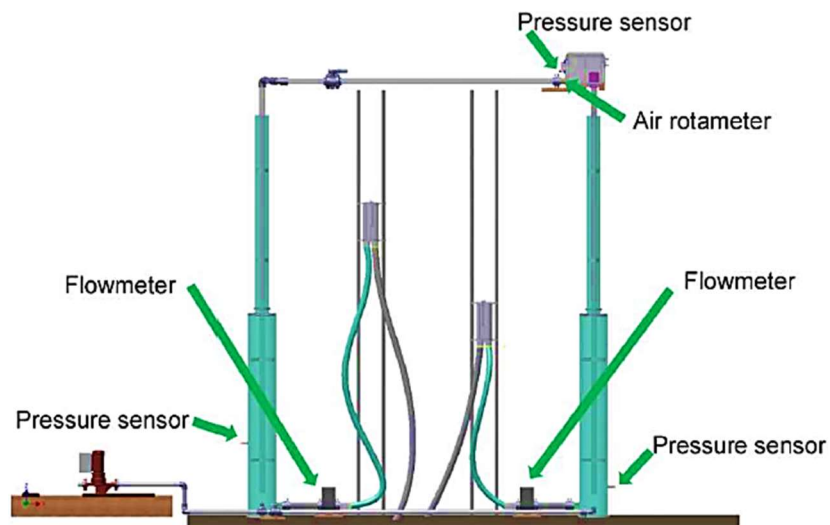


**Figure 7** Instrumentations allocated on the system (Source [10])

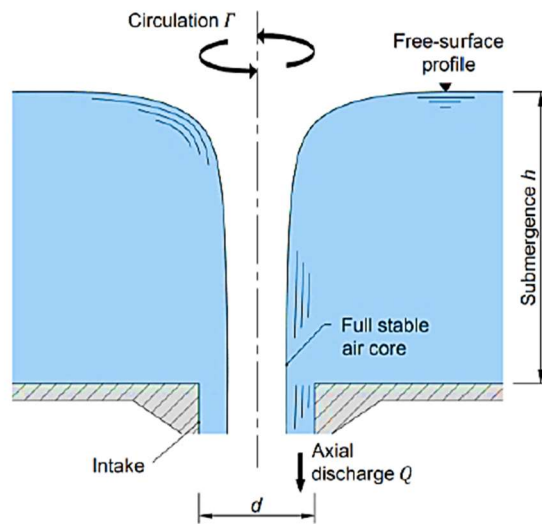


**Figure 8** Schematic of a full air core vortex under strong circulation conditions (Source [13])

As anticipated, the core of the system is the sealed box, located at the end of the horizontal section. In a first moment, it was designed with a parallelepiped shape (Figure 9). The multiphase flow of air and water condition of the siphon is here guaranteed thanks to free-surface vortex, where a concentrated region of vorticity results in a local depression of the free-surface, and under ideal conditions of circulation, air entrainment and flow of air through a full air core is maintained [14]. In the sealed box, an off central vertical orifice (funnel) connected to the downstream vertical pipe ensures a steady rate of vorticity, generated by the asymmetry of the approach flow geometry from the horizontal pipe [13]. In order to provide enough circulation to maintain a stable vortex air core over the outlet, an additional scroll type vortex chamber was added. It was designed according to the depth-discharge equations derived by Mulligan et al. for subcritical approach flows ( $Fr_1 < 1$ ) [15], and it's characterized by a logarithmic spiral geometry (Figure 9).

This configuration allowed to record the discharge from both reservoirs, the pressure inside both reservoirs and inside the box, the air flow inside the box.

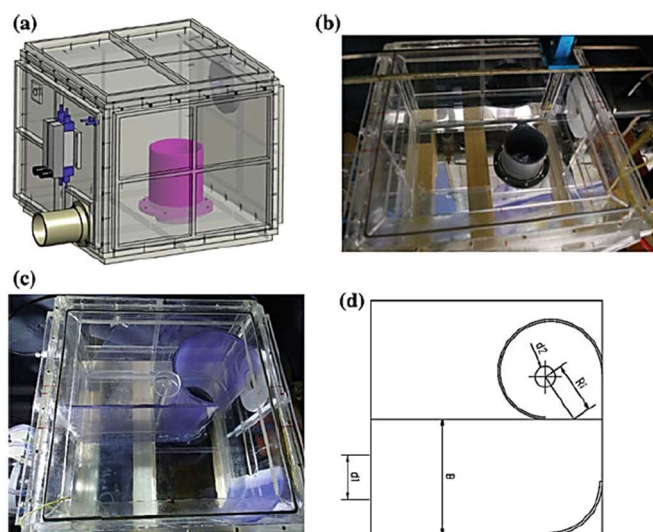


**Figure 9** (a) 3D schematic drawing of the sealed box built in Lab (b) image of the sealed box prototype (c) adaptation with a scroll vortex chamber (d) representation of the spiral geometry (Source [10])

---

## 2.2.2 Parametric studies on vortex chamber

Tests at different pressures were carried out in the sealed box in order to characterize the flow conditions and the depth-discharge relation for two size of funnels (63 and 90 cm).

Results showed a good agreement between the experimental data and the theoretical equations and that this relation is separated by a transition point. The considered theoretical equations were the weir equation, with a discharge coefficient equal to 0.44 (Eq.(2.1)), and semi-empirical vortex equations as defined by Mulligan et al. (Eq.(2.2)) based on the approach flow geometry (see [15]).

$$Q = 0.44\pi\sqrt{2gh^{1.5}} \quad (2.1)$$

$$Q = \frac{k_\alpha}{\left(\frac{5\alpha d}{h}\right)^{n_\alpha}} \sqrt{gd^{5/2}} \quad (2.2)$$

Where:

$$k_\alpha = -0.12\alpha^3 + 0.79\alpha^2 - 0.62\alpha + 0.36 \text{ for } 1.3 \leq \alpha \leq 6.22$$

$$n_\alpha = 0.05\alpha^2 - 0.39\alpha - 0.55 \text{ for } 1.3 \leq \alpha \leq 6.22$$

At atmospheric pressure, for low discharges the weir approach fit well the results as the flow system is independent of the rotating flow conditions. For higher discharges the vortex approach fit well with the data (Figure 10) [10].

If for low discharges similar values were obtained for both diameters, in the other case the diameter of the funnel highly influences the capability of the system to evacuate the water: by increasing the diameter, at the same height corresponds a higher discharge [16].

The same tests were conducted at negative pressures, closing the box in an airtight manner: with the aid of rotameters it was possible to measure the flow of air carried by the flow. The depth-discharge relation showed the same trend obtained in atmospheric conditions (Figure 11) stating that (for the measured conditions) free-surface discharges in weir and vortex flow are independent from pressure and they only depend on gravity and on the approach flow conditions [15].

The influence of air inflow was then investigated, and thus the condition of “loss of prime”.

The study, conducted for weir flow condition, showed how the discharge of the system decreases while air is allowed to enter in the siphon (Figure 12). That reduction, as it is explain in [10], can be approximated by the formula showed in Eq (2.1). The loss of prime will occur when the water discharge is unable to evacuate the air downstream. In particular, this occurs when the axial velocity in the downstream pipe is lower than about 0.4 m/s, that can be related to the buoyant velocity of air bubbles in water [10].

$$\frac{Q_2}{Q_{2i}} = \frac{1}{15} \frac{Q_{air}}{Q_2} \quad (2.3)$$

Where:

$Q_{2i}$ : initial water discharge without air inflow;

$Q_2$ : water discharge when air is allowed to enter into the system;

$Q_{air}$ : air inflow measured at atmospheric pressure.

In conclusion, it can be affirmed that the main air evacuation parameter is the water discharge and that the operating points of the by-pass system are:

- de-priming point due to the incapacity to evacuate air inflow (lower operating limit);
- transition point with flow that changes from radial to vortex;
- submerged point (higher operating limit).

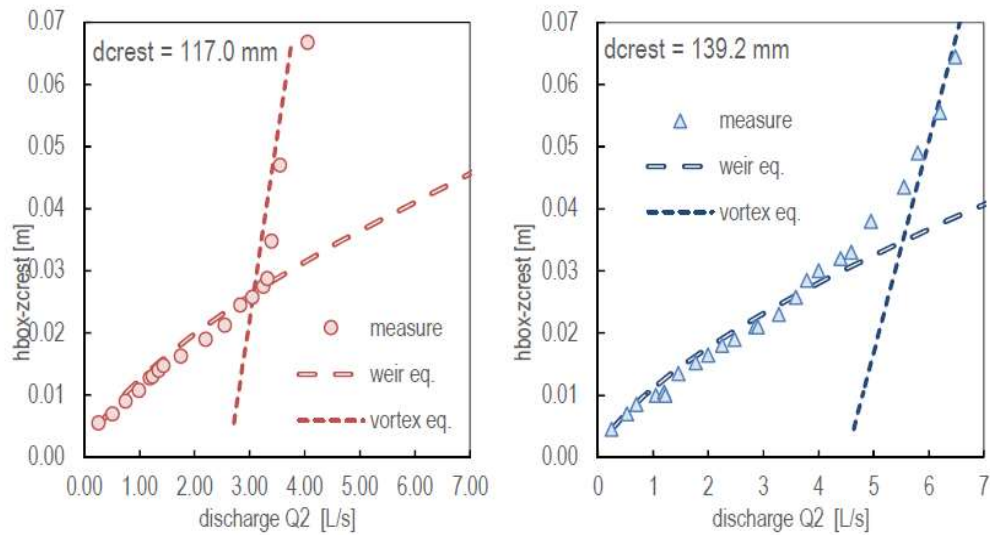


**Figure 10** Depth-discharge relation for two size funnels, 63 cm on the left and 90 cm on the right, under atmospheric pressure (Source [10])

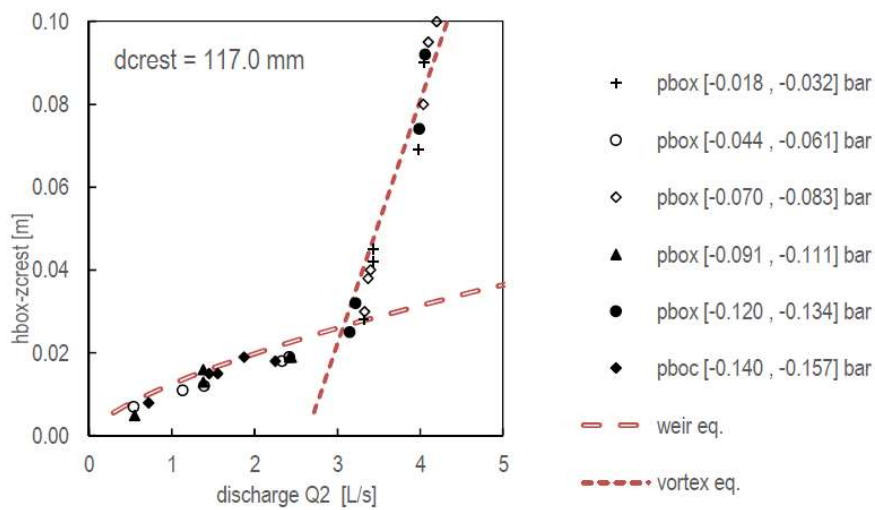


**Figure 11** Depth-discharge relation for the small funnel under variable negative pressure inside the box (Source [10])

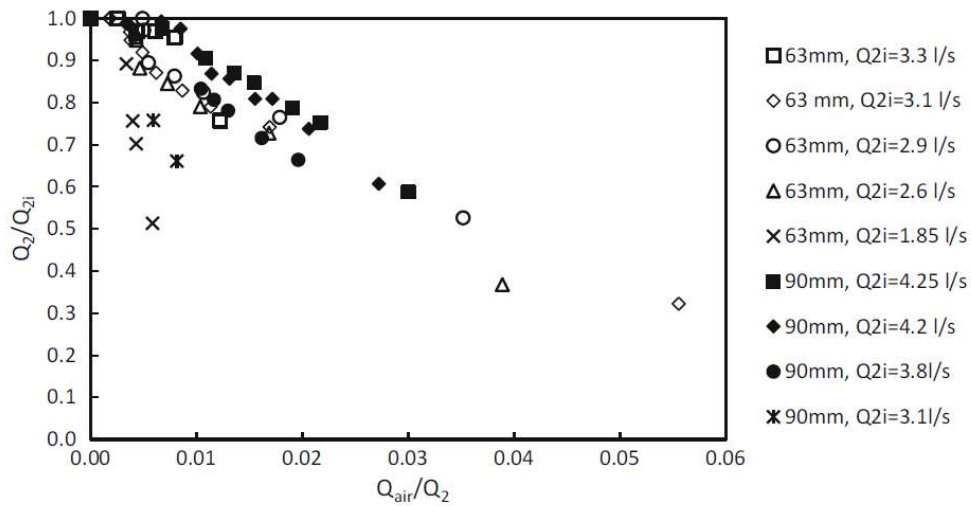


Figure 12 Relative air inflow and discharge reduction, for weir flow condition (Source [10])

The final sealed box installed on field has a cylindrical shape, with a nominal diameter of 400 mm (Figure 14). Same tests, at atmospheric and at negative pressures, were conducted on the new box where, for each mean value of water height registered on it, a value of discharge was associated. Comparing these results with the ones from the first shape box, depth-discharge curves showed a similar behavior seen in the previous model with a parallelepiped shape, (Figure 13, green curve).

The curve showed nevertheless a very quickly switch in the vortex mode, registering a too rapid increase of discharges and a presence of high turbulence. In order to mitigate the sharp rise, a deflector was installed at the entrance of the box [17]. Results showed in this last case a better response (Figure 13, brown curve).

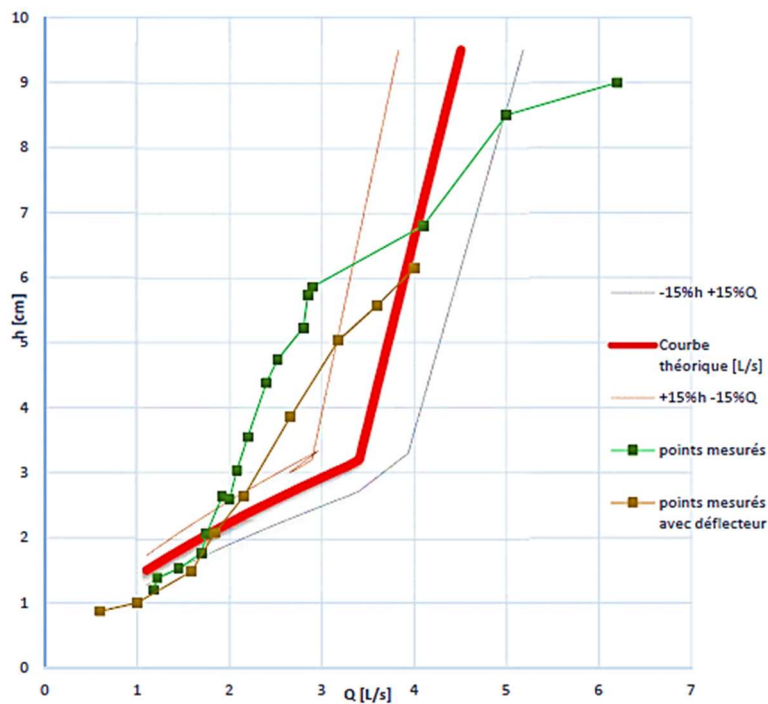
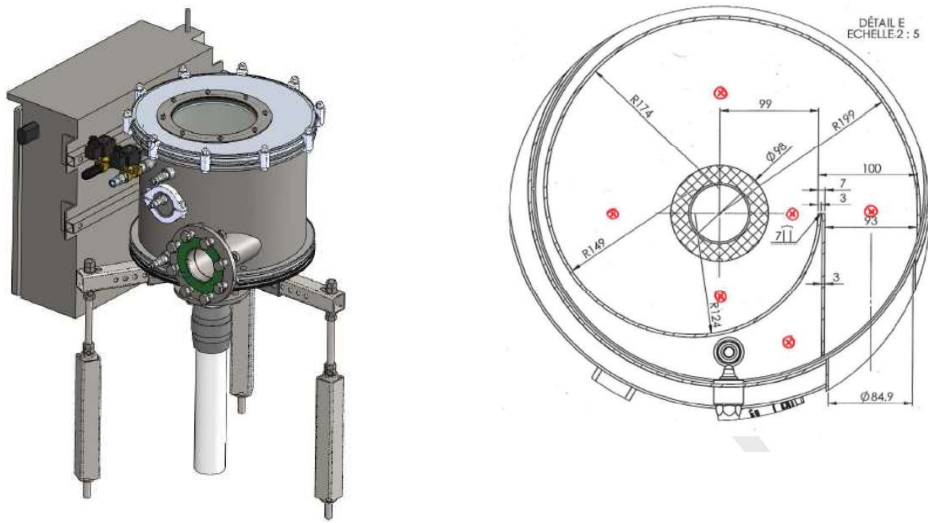


Figure 13 Depth-discharge relation in cylindrical box (Source [17])



**Figure 14** Final shape of the box installed on field

## Chapter 3. Geological and hydrogeological overview

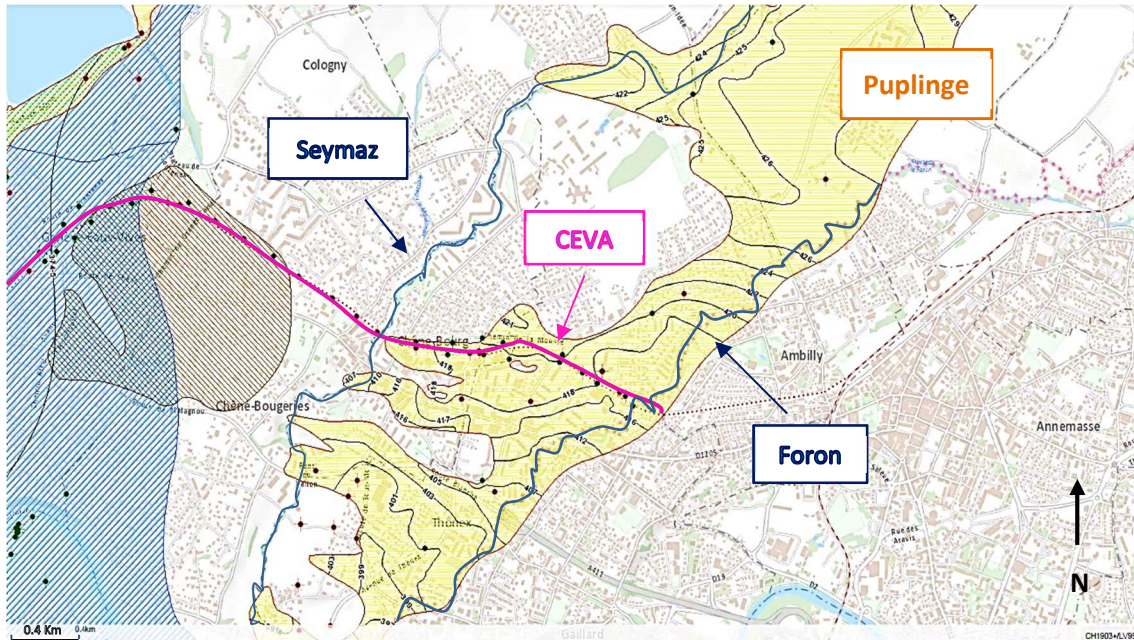


Figure 15 Overall view of Puplinge (Source SITG)

### 3.1 General context

The groundwater object of the study, called “Puplinge”, is an unconfined aquifer with an orientation (NNE-SSW), located between Seymaz and Foron rivers, two Arve effluents (Figure 15). The Swiss portion has a length of 6 km and a width approximately of 1.5 km. It principally flows through a layer of gravel, and a layer of sand, each of them belonging to the Würmien glacial retreat. Part of the gravels were deposited on clayey glacio-lacustrine sediments in the sector of Thônex, and another part on a clayey-silty moraine. The presence of a permeable layer above these clayey units allowed the establishment of the shallow aquifer. The groundwater is mainly fed by rainwater infiltrations. There is no continuous link with the Seymaz, and on the Foron side the river drains the water flow to the south of the railway line, to reaching up to Arve river. [18]

### 3.2 Local context

Before the realization of the tunnel, the flux of the groundwater was from North to South, passing mainly in a transversal direction to the railway cover trench. This is what emerged from the interpretation of hydrogeological data coming from surveys campaigns made from 1959 to 2005. The hydrogeological context is complex, and a general increasing of urbanization during these decades has probably induced modifications on groundwater levels. From the collected data, and by dividing the area of the aquifer into four main zones, it was possible to have a more

detailed idea of the flow directions and the main thicknesses of the aquifer [18]:

- In the area close to the French border (km 73.8 to 74.39), the groundwater flow mainly towards the Foron river. In this area, the thickness of the permeable layer, including the Foron river alluvial deposits, is the most relevant (around 5 meters) and the gradient is the most marked (2 to 3%).
- Further West (km 73.5 to km 73.8), the flow goes more in the North-South direction. The thickness of the permeable layers in this zone is approximately of 2 meters.
- From km 73.2 to 73.5, close Chêne -Bourg station, the flows are directed towards the South/Southwest with an average slope of about 1.5%. The thickness of the permeable layers was estimated to be of 2 meters.
- Close to the Seymaz, the flow directions are less clearly identifiable. Probably, there is low infiltration at the river level. The thickness of permeable layers is locally non-existent and approximately less than 2 meters.

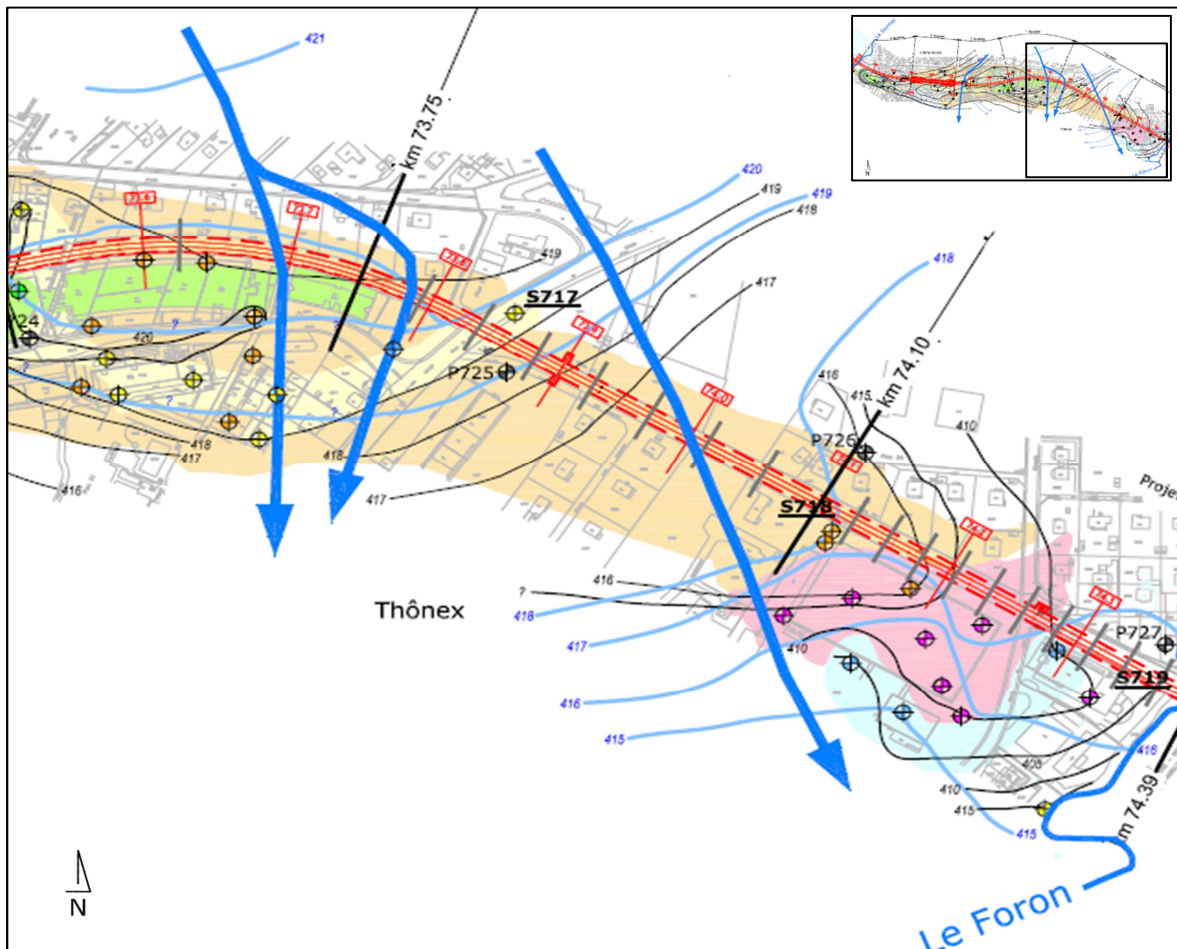


**Figure 16** Main flow directions of the aquifer in the area close to Foron river (Source [18])

**Table 2** Difference of water levels and flow directions in bypasses between 2014-2015 (Source [19])

Considered area	$\Delta H$ [m]	Flow direction
BP01-BP07	from 1.5 to 2.7	N-S
BP08-BP21	from 0.1 to 1.7	N-S
BP22-BP31	from 0 to 2.7	Variab.

In Figure 16, the main Puplinge flow directions in its last section are outlined. It can be seen how water, before the construction of the railway line which is represented in red, was mainly directed toward Foron river.

After the realization of the tunnel, a high difference of water level between upstream and downstream was measured in the same area. Here, the increase of the upstream groundwater level was of the order of 0.5 meters from the beginning of the work and a decrease of the order of 0.2 meters was registered downstream.

In Figure 17, the mean water levels registered before the construction of the tunnel (from 2010 to 2014) were compared with the ones registered in the thirty siphons, in the period of September 2014 to August 2015.

In the area between by-pass BP08 and BP22 the difference of water level, going from upstream to downstream, was lower (0.1 -1.7 m) compared with the others. Here, the increase of the upstream groundwater level was of the order of 0.75 m from the beginning of the project and of the order of 0.3 m downstream.

In the area between BP22 and BP31 the direction of the groundwater flux changed with the time and depending on the area. In some periods the water levels were registered to be higher downstream than upstream. Close to BP25 and BP26 the direction of the water flux seems to be parallel to the railway trench. [19]

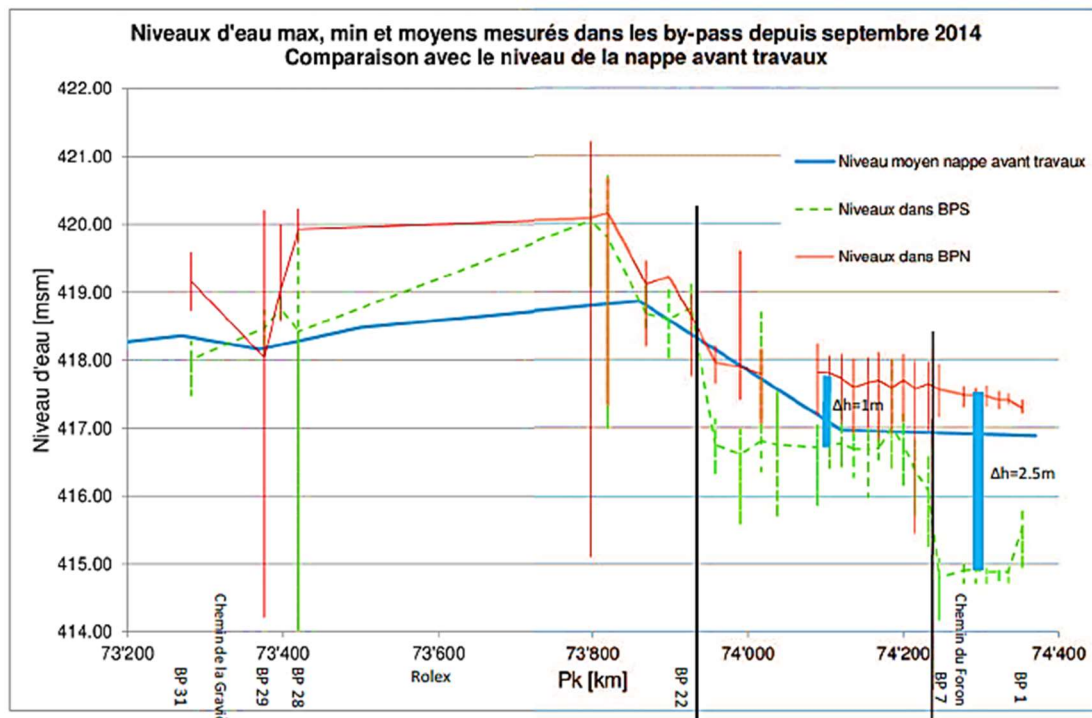


**Figure 17** Comparison between mean water level before tunnel and water levels in upstream and upstream part (Source [19])

In the next two figures, the evolution of water levels registered by two piezometers located in the area close to Foron river are outlined. The first piezometer is located in the downstream part, approximately at 10 meters from the railway tunnel. The second one is placed in the upstream part, at around 60 meters from railway line. In both pictures, after 2014, year of construction of the tunnel, piezometric levels started to increase in the upstream piezometer and decrease in the other one.

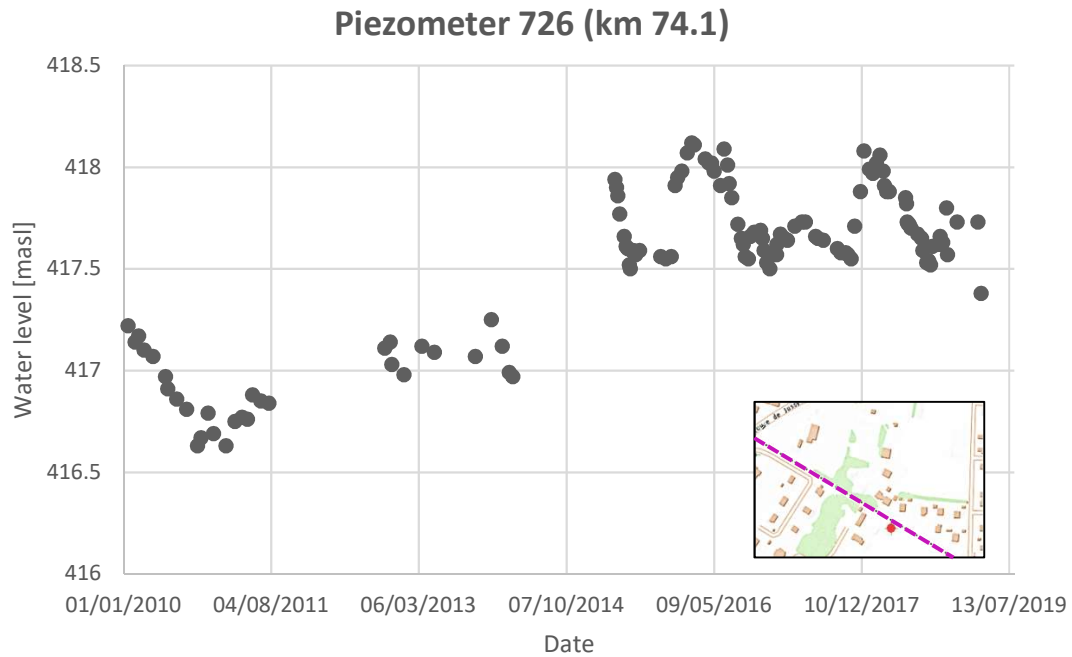


**Figure 18** Variation with the time of water levels in a downstream piezometer

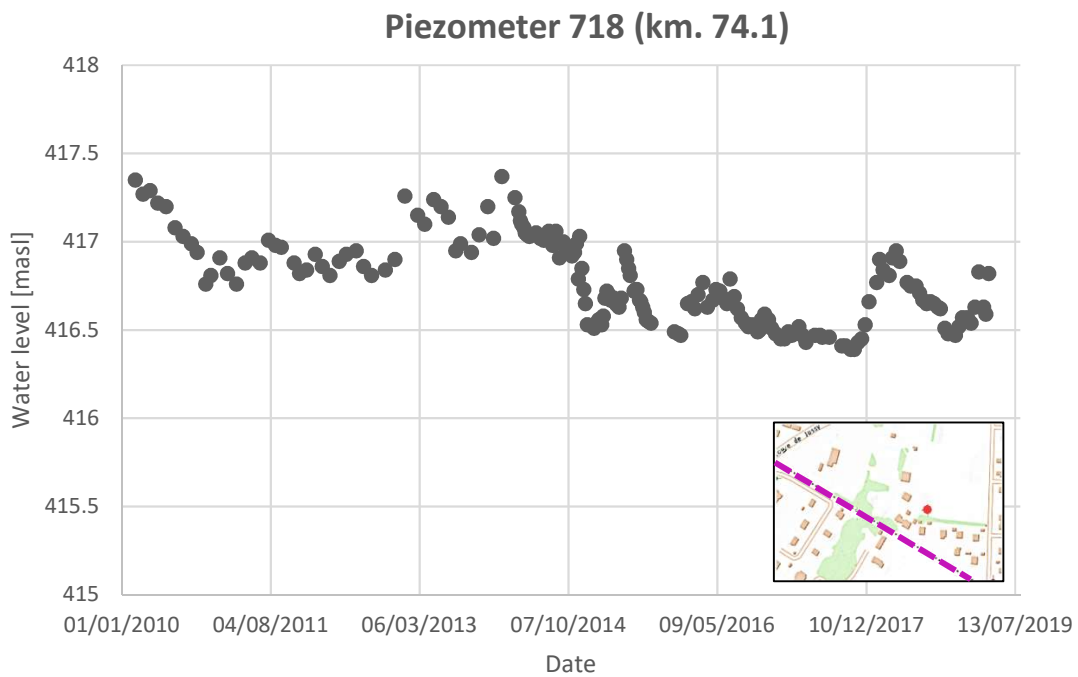


**Figure 19** Variation with the time of water levels in an upstream piezometer

### 3.3 Pumping and infiltration tests

In order to have a response of the behavior of the aquifer and therefore an estimation of the permeability, pumping and infiltration tests were carried out on July 2015 in siphons n.11 and 04, in the area close to Foron river. The analysis was conducted with pumping tests in the upstream part, where water levels are supposed to be higher, and with infiltration tests in the downstream part, where water levels should be lower. Results showed a very local lowering of the aquifer, emphasizing the non-uniformity of the hydrogeological context, with a ray of influence of the order of 30-50 meters (Table 3, Table 4). Low water levels and therefore higher potential difference was encountered. These results can be explained by two main reasons: tests were conducted during summer, and flux in this area is mainly directed through Foron river. Tests showed the necessity to install a drainage trench along the siphons, in order to facilitate capture and infiltration and to limit the water level variations between upstream and downstream, otherwise a lower capability to limit the “cutting effect” by the railway tunnel should be expected. An underestimation of the permeability was consequently noticed. The obtained results showed in fact values of permeability typical of a sand, gravelly sand layers (Table 5). Since groundwater mainly flow through a layer of gravel, a more typical value of permeability would have been of the order of  $10^{-3}$ - $10^{-1}$  m/s [20].

**Table 3** Results from pumping test in BP04 in upstream part (Source [19])

Pumping wells		BPN 02	BPN 03	BPN 04	P751	BPN 05	BPN 06
Distance [m]		25	15	0	5	15	30
Q=21 l/min	ΔH [m]	-0.01	-0.02	-0.47	-0.03	-0.04	-0.01
Q=41 l/min	ΔH [m]	-0.16	-0.19	-1.9	-0.1	-0.09	+0.05

**Table 4** Results from pumping test in BP04 in downstream part (Source [19])

Infiltration wells	BPS 02	BPS 03	BPS 04	BPS 05	BPS 06
Distance [m]	25	15	0	15	30
ΔH [m]	+0.12	+0.36	+0.98	+0.21	+0.01

**Table 5** Values of the estimated permeability (Source [19])

<b>BPN11</b>	$0.5 \cdot 10^{-4}$ m/s
<b>BPN04</b>	$2 \cdot 10^{-4}$ m/s – $9 \cdot 10^{-5}$ m/s
<b>BPS11</b>	$1 \cdot 10^{-4}$ m/s – $3 \cdot 10^{-5}$ m/s
<b>BPS04</b>	$2 \cdot 6 \cdot 10^{-5}$ m/s

### 3.4 Current situation

Nowadays the thirty bypasses built along the railway tunnel in upstream and downstream section work with different principles: some of them work in a gravitative way (from BP 07 to BP10), others are only equipped with piezometers, like BP11, and eight of them have the vortex chamber installed in the downstream part and they work following the siphon principle (Figure 20). These siphons have been built between Chêne Bourg main station and the French border

(km 73.82 to 74.1) and each of them is equipped with automatic piezometers in upstream and downstream part. These systems are currently in operation with a manual prime and measures of water level into the wells are recorded every minute and constantly monitored through VPN system. In a control building located in field, it's also possible to control and change the working conditions of the system (i.e. minimum difference of water level, minimum upstream water level, etc..).

In Table 6, the exact location of the siphons is reported.

**Table 6** Location of the siphons [pKm]

BP11	BP18	BP19	BP20	BP21	BP23	BP24	BP25	BP26
74186	74038	74018	73988	73957	73898	73868	73821	73812



**Figure 20** Left: Siphon in upstream part. Right: Siphon in downstream part, with presence of vortex chamber

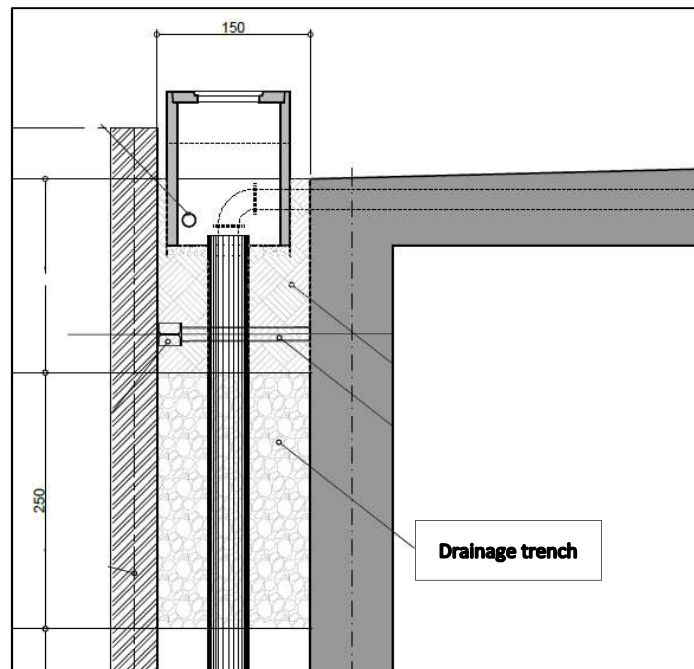


**Figure 21** Schematic representation of upstream part of the siphon system with drainage trench

In order to increase their efficiency, a horizontal drainage trench parallel to the railway tunnel was built along the siphons from BP 24 to BP 18, in the upstream and downstream part. It is made of gravel (high permeability) and it has a height of 250 cm and a width of 150 cm (Figure 21). A more recent visualization of the water levels in the eight siphons is represented in Figure 22. As can be seen, in bypass 23, 24 and 25, water level is higher in downstream than in the upstream part. These siphons are not in operation. Moreover, levels in siphon 11 are quite lower than the others. Collected data of water levels show also a bad connection in bypass 21, with probably an interruption of the drainage trench in the downstream part. Since siphons 18, 19, 20 are the only ones more well connected, this study will be mainly focused on these systems. As will be discussed on the following chapters, these siphons will be the starting point for the assessment of the discharge and the evaluation of the response of drainage trench and aquifer.

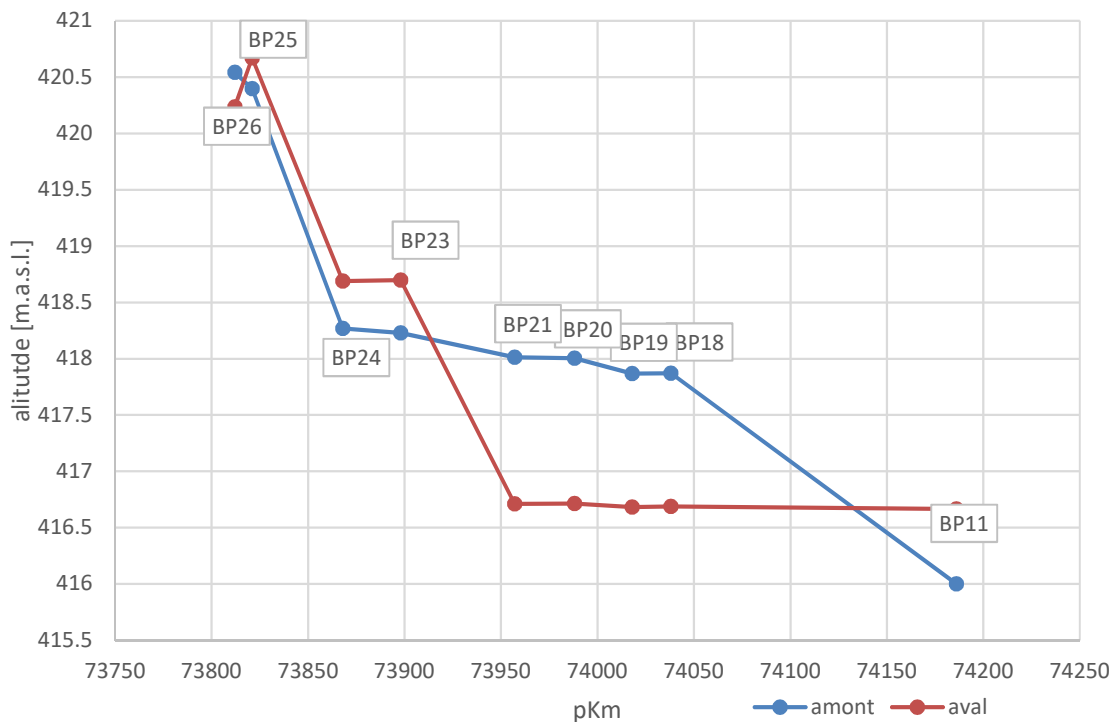


**Figure 22** Visualization of the water levels in siphons on 2 March 2019 at 7.11 am (Source BG)

## Chapter 4. Study of the discharge

In 2017, experiments were conducted on the cylindrical box in order to relate the discharge into the siphon with the water height in the box. Tests, firstly conducted at atmospheric pressure and then in depression, aimed to investigate on: waterflow in the system (with electromagnetic flowmeter), water level in the sealed box (with continuous sonde), depression in the box. For a given difference of water level in the two reservoirs, flow into the system as well as the water height and pressure into the box were investigated. The system was dimensioned in order to convey water with a flow no higher than 5 l/s. Two diameters of the funnel were considered, 63 and 90 mm, and the following steps were performed [17]:

- Setting of water levels into reservoirs;
- Priming of the system with vacuum pump;
- Stop priming when water level in the box reaches the high level;
- Measurements of water level and pressure in the box and flow in the siphon once the water level stabilized for 20 minutes;
- Introduction of air until the siphon is defused;
- Iteration by changing the water levels.

### 4.1 Estimation of water level-discharge relationship on the prototype

Through the experiments conducted in 2017, it was possible to assess the relationship between discharge and difference of water height in upstream and downstream reservoirs. In order to obtain a more realistic result, the average couple of values  $Q-\Delta H$  was considered for each iteration (Table 7). Results are represented in Figure 23, where the two graphs, expressed with a power trendline, show the behavior for both diameters.

**Table 7** Experiments conducted on the system in 2017 (Source: BG)

heure	N_am [mmCe]	N_av [mmCe]	DH [m]	temps [s]	N_box [cm]	h_tulipe [cm]	P_box [mmCe]	Q_siphon [L/s]	commentaires
petite									
	4110	2450	1.66				-2250	2.9	ennoiment rapide
13h00	3965	3555	0.41	0	19.54	2.04	-2273	1.55	H_mid
	3920	3599	0.321	60	20.75	3.25	-2336	2.21	
	3928	3604	0.324	180	21.51	4.01	-2352	2.31	
	3935	3608	0.327	300	21.78	4.28	-2359	2.39	
	3935	3617	0.318	600	21.9	4.4	-2352	2.35	
	3936	3619	0.317	900	21.88	4.38	-2360	2.38	Etat final stable
	3965	3555							H_min => désamorçage
13h45									
	3970	3732	0.238	0	19.05	1.55	-2253	1.43	H_mid
	3956	3738	0.218	60	19.5	2	-2279	1.77	
	3977	3744	0.233	300	19.65	2.15	-2295	1.84	
	3965	3747	0.218	600	19.6	2.1	-2288	1.79	
	3962	3747	0.215	900	19.4	1.9	-2287	1.79	Etat final stable
14h10									
	3975	3802	0.173	0	19.05	1.55	-2248	1.28	
	3968	3811	0.157	120	18.98	1.48	-2258	1.47	
	3964	3811	0.153	300	19	1.5	-2253	1.51	
	3968	3809	0.159	600	19.04	1.54	-2258	1.5	
	3970	3813	0.157	900	18.98	1.48	-2259	1.51	

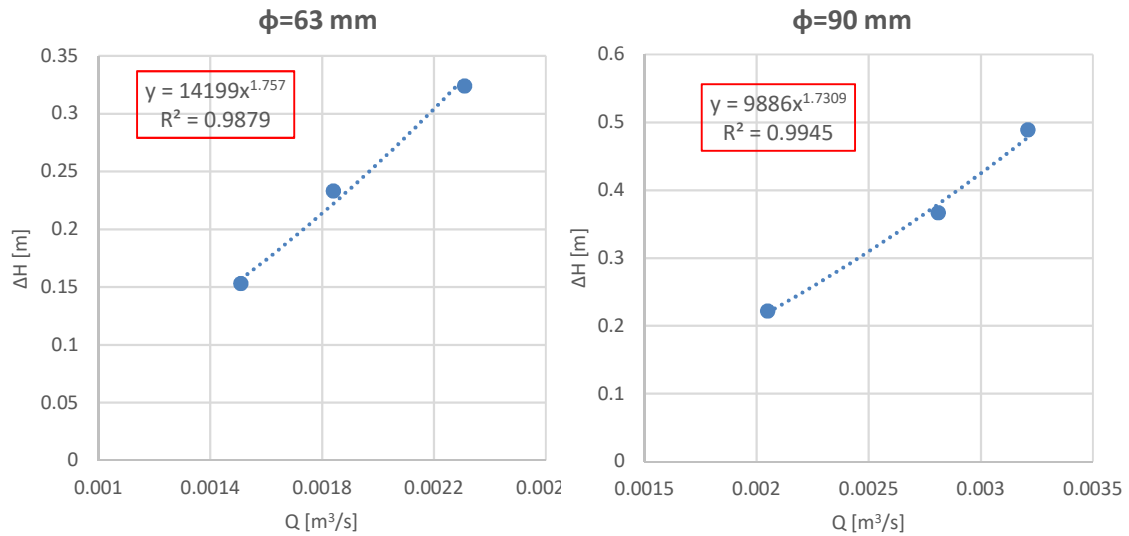


**Figure 23** Difference of water level-discharge relationship with experimental approach

In fluid-dynamics, the empirical relation that link the head losses, along a given length of pipe, with the average velocity of the fluid flow is the Darcy-Weisbach equation, expressed below [21]:

$$\Delta H = h_f + h_{loc} \quad (4.1)$$

$$\Delta H = \frac{fL}{D} \frac{v^2}{2g} + \sum k_i \frac{v^2}{2g} \quad (4.2)$$

Where:

$h_f$ : friction head losses;

$h_{loc}$ : local head losses;

$f$ : friction factor;

$L$ : length of pipe;

$D$ : diameter of pipe;

$k$ : sum of the local head loss coefficients.

Friction head losses predict losses due to fluid friction on the pipe wall and the effect of fluid viscosity [22]: its friction factor ( $f$ ) depends on the type of pipe (shape and roughness) and on the flow properties (laminar or turbulent). Local head losses mostly take into account the presence of bends, fittings and transitions. Although they are generally termed “minor losses”, for relatively short pipe systems they could account for a major portion of head losses.

Overall, head losses depend on the square of the velocities since they represent energy dissipations related to turbulence phenomena and therefore they have to be similar to the ones typical of turbulent motion [23].

Rewriting Eq. (4.2) in terms of discharges, the equation becomes:

$$\Delta H = \frac{16}{\pi^2 D^4} \cdot \left( \frac{fL}{2gD} + \frac{\sum k_i}{2g} \right) \cdot Q^2 \quad (4.3)$$

$$\Delta H = K \cdot Q^2 \quad (4.4)$$

The equations represented in Figure 23 have values of the exponent equal to 1.757 for a diameter of 63 mm, and a value equal to 1.73 for a diameter equal to 90 mm. Raising to the square the values of discharges obtained in Figure 23, a Darcy-Weisbach relationship was obtained, and it's showed in Figure 24.

Analytical and experimental equations were both compared in Figure 25 for a diameter of 90 mm. Results indicate a very low difference between the two approaches.

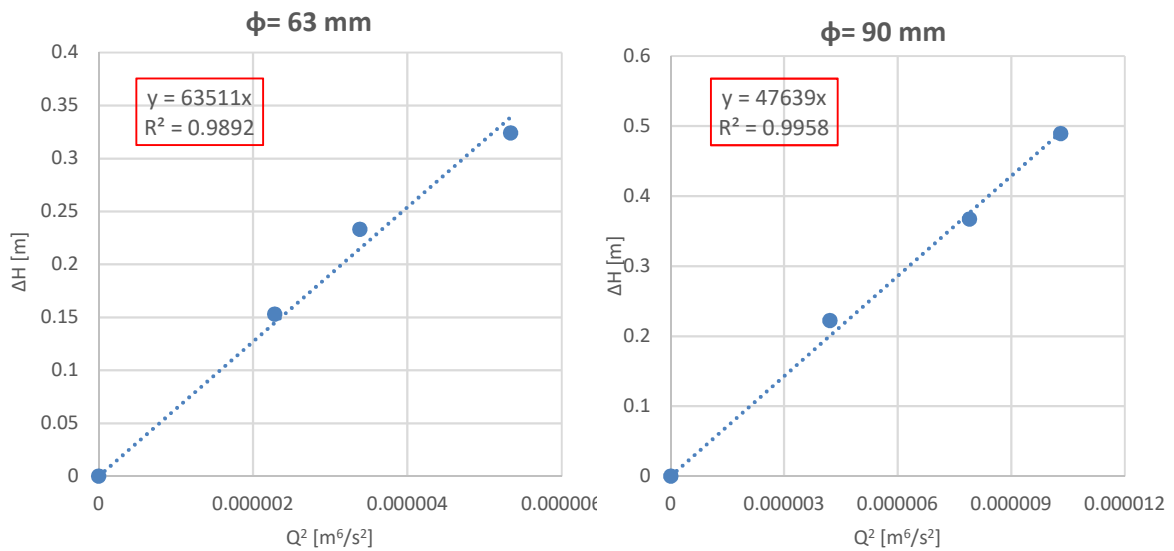


Figure 24 Difference of water level-discharge relationship with analytical approach

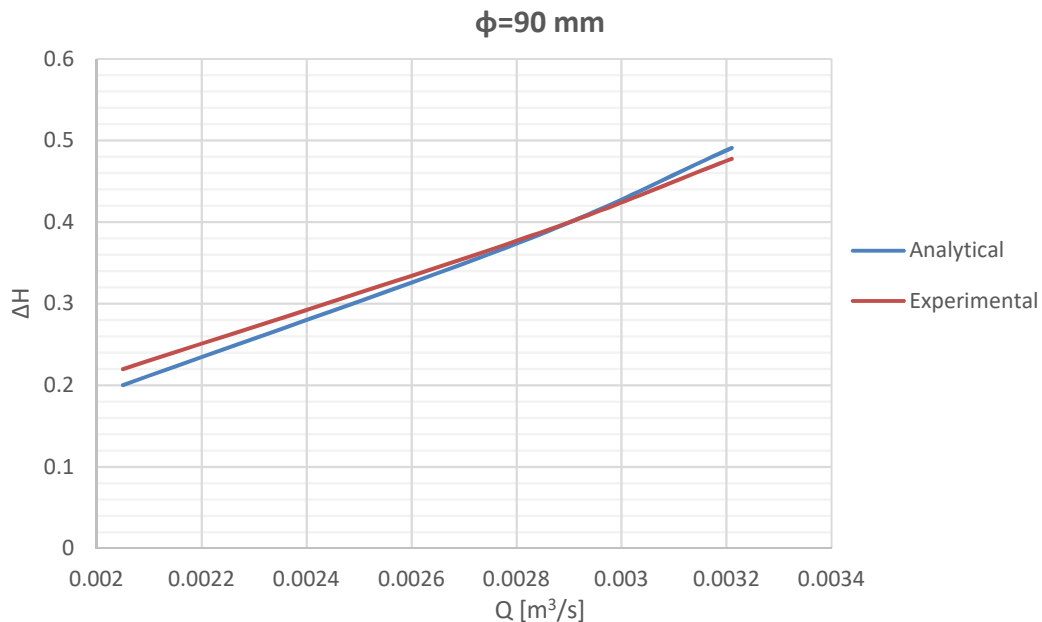


Figure 25 Comparison between analytical and experimental approach

## 4.2 Discharge estimation on the siphons in situ

Due to the high influence of the size diameter to evacuate air inflow in the downstream part, the final groundwater transfer system was built with a pipe diameter of 90 mm. Next results are therefore always referred to this case.

Since first measurements of water levels recorded by the piezometers in the siphons are available, the discharge fluxing from upstream to downstream was estimated in siphons 18, 19, 20 by using the analytical formula (Eq. (4.5)).

$$\Delta H = 47639Q^2 \quad (4.5)$$

### 4.2.1 Results

Values of outflow were examined during manual pumping tests: siphons are in testing phase and manual priming tests are being conducted in order to assess the response of the systems. Results (Appendix B) showed a similar range of values in the three siphons, with discharge values close to 5 l/s, as it was assumed in the model study phase. An example is given in Figure 26, where values of outflow in siphon n.18 are represented, referring to the pumping test conducted from 08/02/2019 to 04/04/2019. The reason why this period was chosen is because, so far, it's the one in which higher values of difference of water levels, and therefore higher discharge, were registered. After this period, for the exception of intensive rain events, difference of water levels between upstream and downstream wells decreased and got stabilized, proving that, at well-scale, siphons are working in the right way.

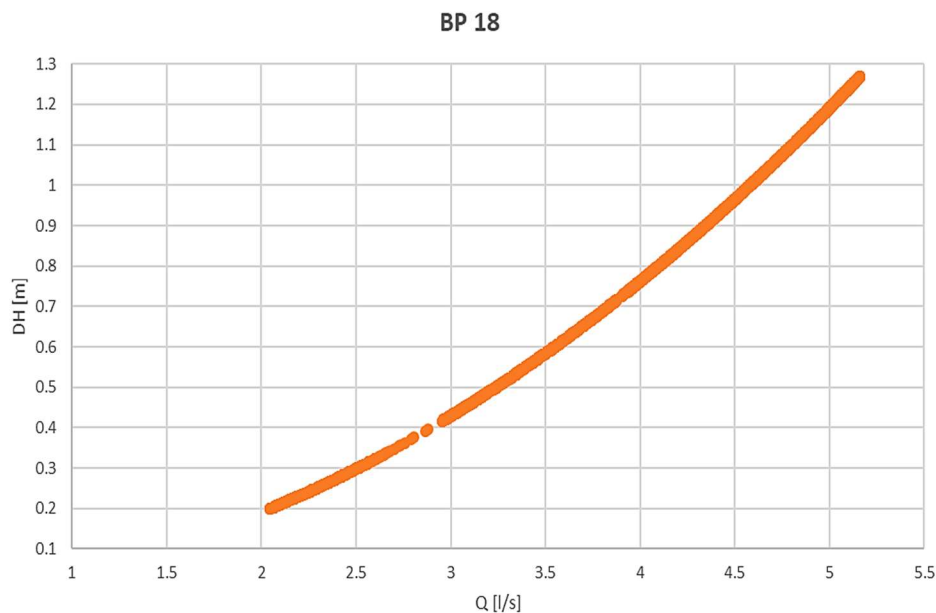


**Figure 26** Analytical discharges assessed in BP 18 in the period of February-March 2019



**Figure 27** Pumping test conducted in BP 18 from 08/02 to 21/02

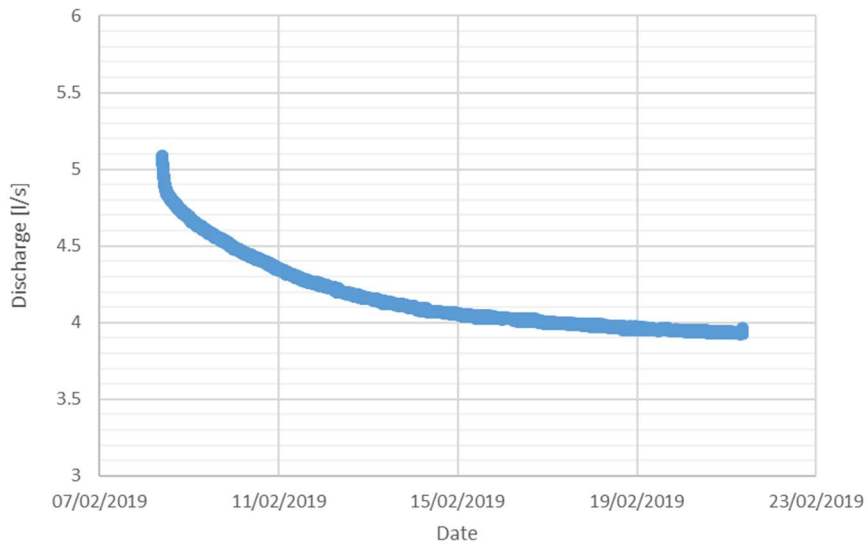


**Figure 28** Outflow in BP 18 during pumping test from 08/02 to 21/02

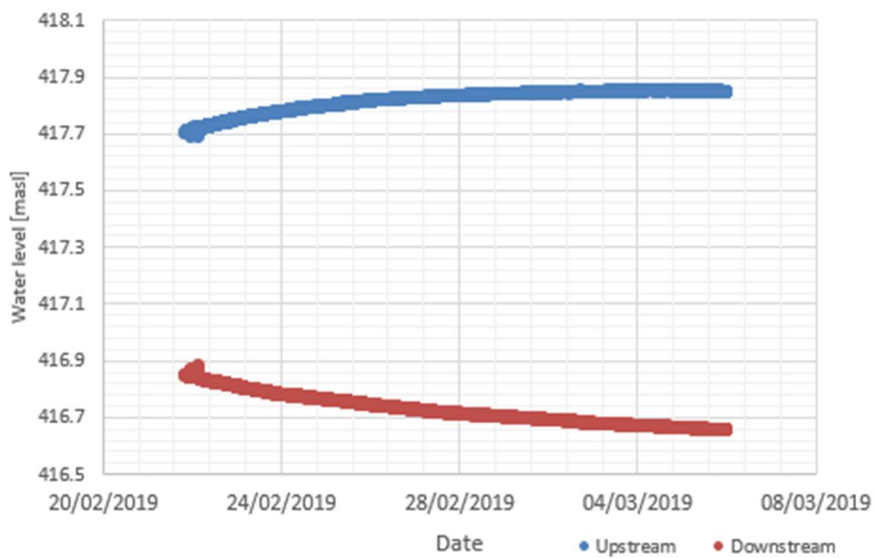


**Figure 29** Response of BP 18 after the depriming on 21/02

Considering the specific pumping test conducted simultaneously on the three siphons from 08/02/2019 to 21/02/2019, the evolution of the water levels in upstream and downstream wells was monitored and results are outlined in Figure 27 by referring in particular to siphon 18. Knowing the evolution in time of difference of water levels ( $\Delta H$ ), pumping test allowed to assess the flowrate in the three bypasses. Figure 28 shows the values of discharge obtained in siphon n.18. In each siphon, a decrease of the upstream water levels of the order of 0.26 meters was registered, and therefore a similar increase of the downstream water level was obtained. After the defusing, as it is expected, difference of water levels started to increase again. Bypass 18 took approximately 12 days to reach again the stability, with a value of the upstream level equal to 417.84 m.a.s.l. and 416.65 m.a.s.l. in downstream part (Figure 28).

### 4.3 Estimation of fitting and local head losses

Distribution of fitting and local head losses was assessed by means of Eq. (4.3) and Eq. (4.5). Results were obtained by considering an equivalent sand roughness  $K_s$  equal to  $1.5 \cdot 10^{-6}$  meters, typical value for pipes in PVC (see [24]). Friction factor ( $f$ ) was calculated through Coolebrook equation, valid for turbulent flow [23]:

$$\frac{1}{\sqrt{f}} = -2 \log_{10} \left( \frac{k_s/D}{3.7} + \frac{2.51}{Re\sqrt{f}} \right) \quad (4.6)$$

$$Re = \frac{VD}{\nu} \quad (4.7)$$

Where:

$f$ : friction factor [-]

$k_s$  [m]: relative sand roughness of the pipe;

$D$  [m]: diameter;

$Re$ : Reynolds number;

$V$  [m/s]: velocity;

$\nu$  [m<sup>2</sup>/s]: kinematic viscosity of water ( $1 \cdot 10^{-6}$  m<sup>2</sup>/s at 20°C).

Local head losses were obtained through the difference between total head losses and friction head losses. As it is depicted in Table 8, local head losses are big if compared with the friction head losses, arriving to be almost five times bigger when the discharge is equal to 5 l/s. In particular, knowing the value of discharge and diameter (90 mm), through Eq. (4.8), it can be easily assessed that the sum of the local head coefficients ( $\sum K_i$ ) is equal to 30.

$$h_{loc} = \frac{16}{\pi^2 D^4} \frac{\sum k_i}{2g} Q^2 \quad (4.8)$$

A typical value of fitting head loss coefficient at the entrance of the water well screen pipe is not lower than 1.43 (see [25]), and at the exit is not lower than 2.8. Considering also that the 90 degree miter bend located in the left part has a coefficient around 1.1, it can be affirmed that head loss coefficient provided by the vortex chamber is the most relevant. In the sealed box, a full air core vortex creates turbulence dissipating a high amount of energy coming from the siphon system. In this way, the siphon system supply the vortex process which in turn dissipates

high part of the available energy, allowing to convey water and air in the downstream part.

**Table 8** Distribution of frictional head losses and local head losses

Q [l/s]	1	2	3	4	5
Re [-]	14147	28294	42441	56588	70736
f [-]	0.0283	0.024	0.0219	0.0205	0.0196
$h_f$ [m]	0.011	0.037	0.077	0.128	0.191
$h_{loc}$ [m]	0.037	0.151	0.34	0.604	0.945
$\Delta H$ [m]	0.047	0.188	0.416	0.732	1.135

In order to have a further proof of how the vortex influences head losses distribution, an assessment was conducted by considering the same siphon system without the vortex chamber: it was considered to have the same fitting head losses coefficient and the entrance and at the outlet and that it's constituted by 90 degree miter bends in the two corner in the up part. In this case, the sum of local head coefficients ( $\sum K_i$ ) was found to be around 6.43. Estimating, in function of the discharges, the new values of head losses (Appendix A), a new water level-discharge relation was obtained:

$$\Delta H = 15937Q^2 \quad (4.9)$$

In this case, it can be assessed how, at a given difference of water level ( $\Delta H$ ), a higher flow rate is needed. For example, considering a  $\Delta H$  equal to 0.5 meters, by means of Eq. (4.5) a value of Q equal to 3.24 l/s would have been obtained. Applying Eq. (4.9) and therefore considering the case without vortex chamber, a value of discharge equal to 5.6 l/s would have been achieved.

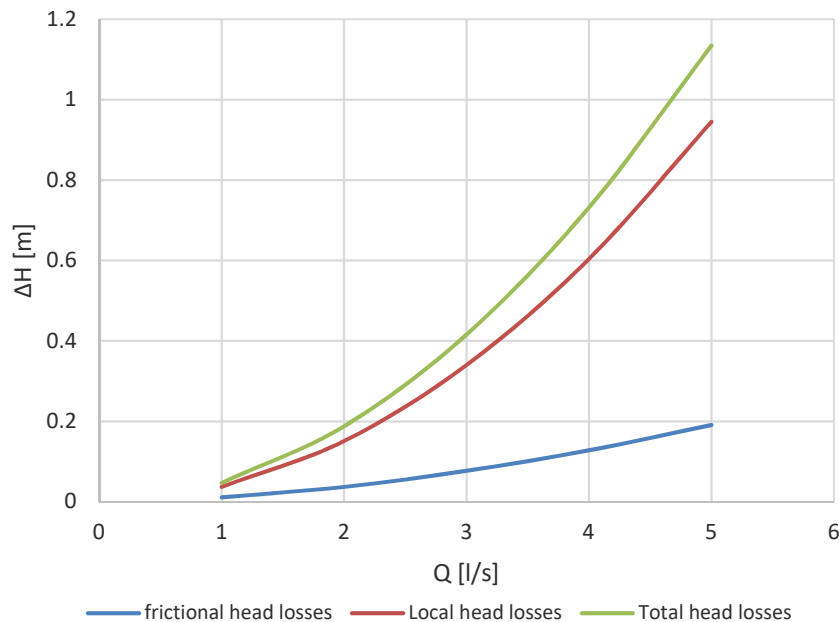


**Figure 30** Distribution of head losses in siphon system with vortex chamber

---

## Chapter 5. Analytical study of the drainage trench

The drainage trench is an artificial system, realized with the purpose of increasing the efficiency of the siphons in the reconnection of the aquifer, more specifically in the process of withdrawal and infiltration. It is placed in a longitudinal way, from bypass 18 to 24, in upstream and downstream part. It is made of gravel (high permeability) and it has a constant thickness of 2.5 meters and a length of 1.5 meters from the railway walls.

Once outflow in siphons has been estimated, the second step was to study the response of the aquifer along the three siphons (18 19 20), and therefore along the drainage trench, while water levels are getting lower in the upstream wells and increasing in those in downstream part. A 1D analytical approach was adopted.

In Figure 31, evolution of the water levels in the three siphons from 01/02/2019 to 13/05/2019 is represented. So far, three pumping tests were mainly conducted, and it can be seen how immediate the response of the aquifer in the wells is: at a decrease of water levels in upstream part, it immediately corresponds an increase in the downstream part.

In order to estimate the response of the drainage trench, the main theoretical concepts related to groundwater flow are presented in paragraph 5.1. Then, the main assumptions for the estimations of the lowering/rises in the drainage trench are presented. Finally, results are showed and discussed.

### 5.1 Analytical solutions of differential flow equation

The differential flow equation governs the distribution of the motion field in the groundwater system. It's an expression of the law of conservation of mass and head losses:

$$\nabla \cdot (\rho v) = -\frac{\partial}{\partial t}(\rho n) \quad (5.1)$$

$$v = -K \cdot \nabla h \quad (5.2)$$

$$\frac{\partial}{\partial t}(\rho n) = \rho S_s \frac{\delta h}{\delta t} \quad (5.3)$$

Where:

v= filtration velocity;

$\rho$ = density of water;

n= porosity;

K= tensor of hydraulic conductivities;

$S_s$ = specific storage coefficient.

For unconfined aquifers and in transient conditions, the differential flow equation is:

$$\nabla^2 h = \frac{S_y}{T} \cdot \frac{\delta h}{\delta t} \quad (5.2)$$

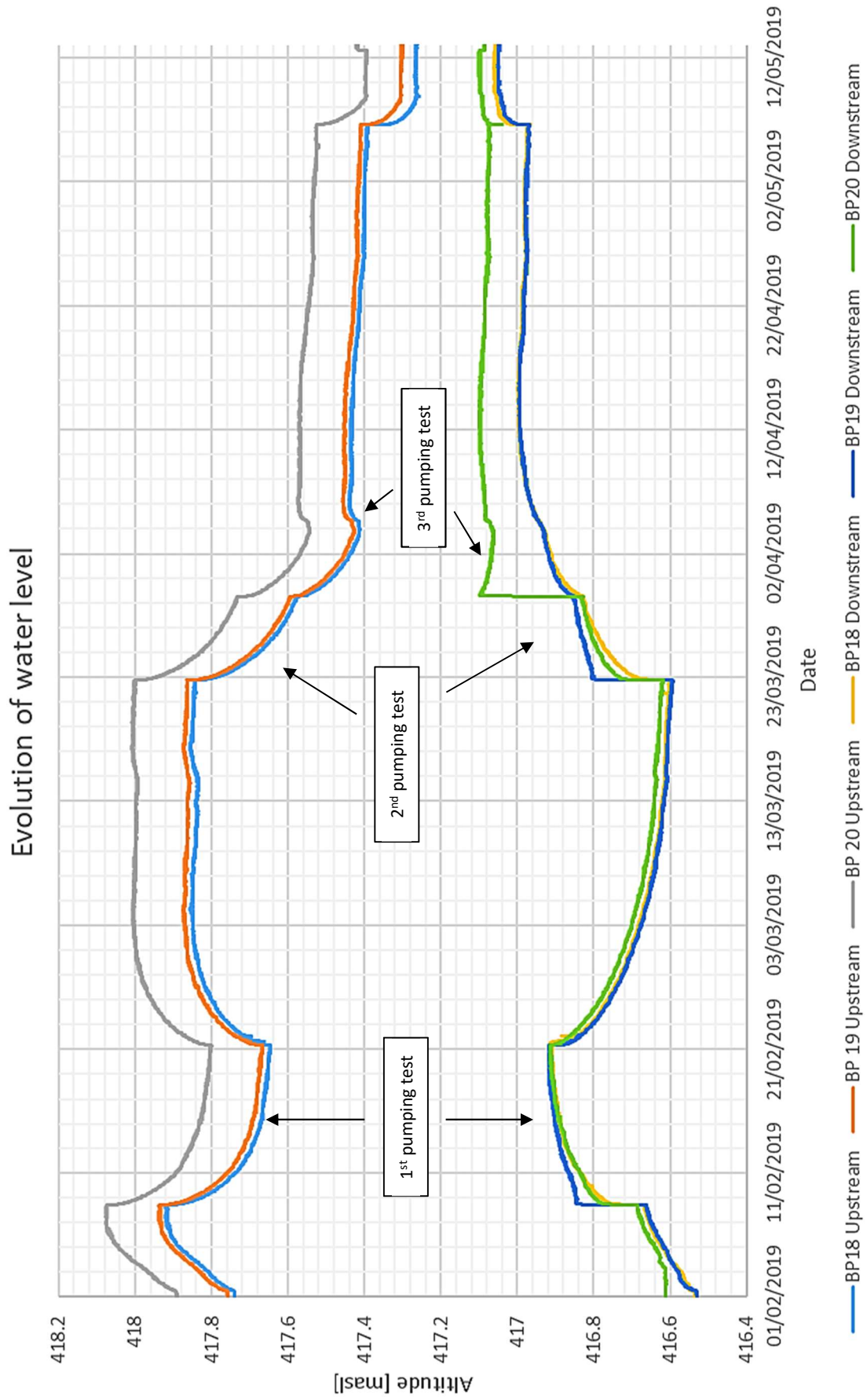


Figure 31 Evolution of water levels in BP 18,19,20 from 01/02/2019 to 13/05/2019

---

$$\frac{\partial^2 h}{\partial r^2} + \frac{1}{r} \frac{\partial h}{\partial r} = \frac{S_y}{T} \frac{\partial h}{\partial t} \quad (5.3)$$

Where:

$S_y$ : specific yield [-]

T: transmissivity [ $m^2/s$ ]

r: distance from well [m]

Eq (5.3) is developed by considering a radial system, which is the flow geometry mostly adopted for analyzing well-aquifer flow problems. It's a particular 2D geometry where flow lines are rectilinear and they converge towards the well axis, with a identical configuration independently by the altitude (Figure 32). Radial flow geometry can be applied only if some conditions are simultaneously respected [26]:

- Aquifer has infinite areal extent;
- Aquifer is homogenous and of uniform thickness;
- Screen well is fully penetrating;
- Flow to screen well is horizontal when screen well is fully penetrating;
- Water is released instantaneously from storage with decline of hydraulic head;
- Diameter of pumping well is very small so that storage in well can be neglected.

Eq (5.3) represents the same differential equation used for confined aquifers, where the specific yield ( $S_y$ ) has replaced the storage coefficient (S). Specific yield, also known as drainable porosity, represents the volume of water released from a representative saturated sample of aquifer, under the effects of the only forces of gravity. Storage coefficient, or storativity, is the volume of water released from storage per unit decline in hydraulic head in the aquifer, per unit area of the aquifer. For unconfined aquifers, storativity is approximately equal to the specific yield, since the only atmospheric pressure, and therefore the only force of gravity is involved [20].

The reason of using the same equation of confined aquifers is explained by the hydrodynamic behavior of an unconfined aquifer, which is characterized by three main steps:

- a) At the beginning, the water supply is based on the elastic storage of the aquifer, similarly to a confined aquifer;
- b) The second phase is generally called "delayed gravitational drainage", where the increase of lowering tends to reduce;
- c) In third phase, lowering start to increase again, based on the value of the specific yield  $S_y$ .

The duration of the first two phases depends on the granulometry and therefore on the permeability and homogeneity of the aquifer. In any case, if the study doesn't involve the first transitory phase, phase a) and b) can be neglected and differential equation valid for confined aquifers can be considered.

Since high times are considered in this case-study, solutions can be found by treating the system in long-term transitory period.

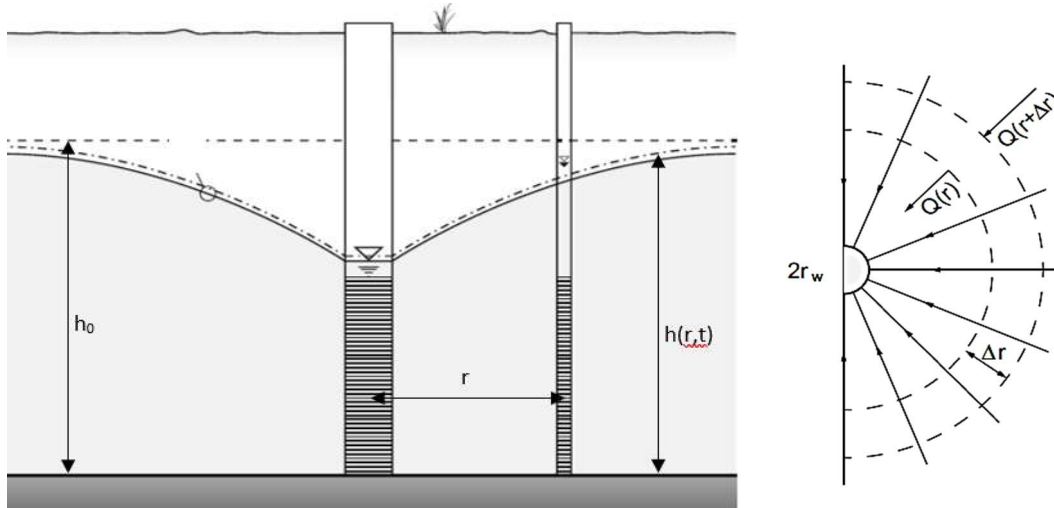


Figure 32 Schematic representation of radial flow geometry referred to an unconfined aquifer (Source [20])

The initial and boundary conditions of equation (5.3) are:

$$h(r, 0) = h_0 \quad (5.4)$$

$$h(\infty, t) = h_0 \quad (5.5)$$

$$\lim_{r \rightarrow 0} \left( r \frac{\partial h}{\partial r} \right) = \frac{Q}{2\pi T} \quad \text{for } t > 0 \quad (5.6)$$

The solution, developed by Charles Vernon Theis (1935), is:

$$s(r, t) = h_0 - h = \frac{Q}{4\pi T} \int_u^\infty \frac{e^{-u}}{u} du \quad (5.7)$$

$$u = \frac{Sr^2}{4Tt} \quad (5.8)$$

Many times, the integral in equation (5.7) is symbolically represented by  $W(u)$ . The drawdown  $s(r,t)$  can then be written as:

$$s(r, t) = \frac{Q}{4\pi T} W(u) \quad (5.9)$$

Values of  $W(u)$  are tabulated in [27]; they can be evaluated through the series development of the exponential integral:

$$\int_u^\infty \frac{e^{-u}}{u} du = W(u) = \left[ -0.5772 - \ln(u) + u - \frac{u^2}{2 \cdot 2!} + \frac{u^3}{3 \cdot 3!} - \frac{u^4}{4 \cdot 4!} \dots \right] \quad (5.10)$$

For low values of  $u$ , such that  $u \leq 0.02$  (i.e.  $\frac{Sr^2}{4Tt} \leq 0.02$  and  $t \geq 12.5 \frac{Sr^2}{4Tt}$ ), and how is expressed in Table 9, the series development could be stopped at the first two terms:

$$W(u) = -0.5772 - \ln(u) = -\ln(1.781 \cdot u) = \ln \frac{1}{1.781 \cdot u} \quad (5.11)$$

Consequently, This equation can be expressed as:

$$s(r, t) = \frac{Q}{4\pi} \ln \left( 2.25 \frac{T \cdot t}{S r^2} \right) \quad (5.11)$$

$$s(r, t) = 0.183 \cdot \frac{Q}{T} \log \left( 2.25 \frac{T \cdot t}{S r^2} \right) \quad (5.12)$$

Eq (5.11) and (5.12) are known as Jacob equations and they show how lowering of the piezometric level increase with respect to the time with a logarithmic law. They are valid in constant flow rate conditions. [20]

**Table 9** Minimum times for application of logarithmic Jacob approximation for unconfined aquifers. If not differently specified, times are expressed in hours (Source [20])

$r$ (m)	$T = 10^{-2} \text{ m}^2/\text{s}$		$T = 10^{-4} \text{ m}^2/\text{s}$	
	$n_e = 0.1$	$n_e = 0.3$	$n_e = 0.1$	$n_e = 0.3$
10	3.5	10.4	347.2	1041.2
50	86.8	260.4	8680.6	26041.7

## 5.2 Estimation of groundwater levels evolution

Siphons 18, 19, 20 are currently in working conditions, monitored through manual primings. How it is showed in Figure 31, three main pumping tests were conducted from 08/02/2019 to 13/05/2019 in the three bypasses, for a duration indicated in Table 10.

In order that all the conditions at the basis of Theis equation were respected, every pumping test was divided in small time ranges. The aim was to consider values of outflow the most constant possible, with the purpose of obtaining response of the aquifer much more realistic. When valid conditions were found, Jacob equation was adopted. For each considered point, the total lowering was obtained by the sum of the contribution of lowering coming from each well, with distances changing for each point (overlapping principle effects). Same principle was adopted for the estimation of water rise in the downstream part.

The thickness of the permeable layer, at least in the investigated area, and in accord with hydrogeological studies treated in Chapter 3, was estimated to be of 5 meters. In particular, close to siphon system, the first 2.5 meters are made of gravel (drainage trench) and the others 2.5 meters are mostly made of gravel-sandy-gravel material. According to Di Molfetta and Sethi [20], values of permeability of the order of  $10^{-2} - 10^1 \text{ m/s}$  should be expected in the drainage trench and of the order of  $10^{-3} \text{ m/s}$  in the real aquifer.

The most used method for the estimation of hydraulic conductivity and transmissivity of an aquifer is the Cooper-Jacob method (1946). Deriving from Theis equation, this solution aims to determine the most important hydrogeological parameters matching a straight line to drawdown data plotted as a function of the logarithm of time [28]. For the application of this method, all the conditions presented in Theis equation must be also respected.

In the long term, lowering registered in a siphon well with the automatic piezometer is not only generated by the pumping of that specific siphon, but it is also influenced by the pumping tests

conducted at the same time in the other siphons. Moreover, during a pumping test, the three siphons can have different values of discharge. In these conditions, the use of Cooper-Jacob equation was found to be of not easy application. A simplified way was adopted for the estimation of permeability and transmissivity. A first indicative value was chosen, in order to estimate lowering, and also the rising, in all the drainage trench. Then, more realistic values were obtained in an iterative way, until that total lowering, assessed in the three upstream wells, matched the ones registered by automatic piezometers located in each siphon.

**Table 10** Pumping/Infiltration tests conducted on BP18,19,20

Test	Date	Duration
1	From 08/02 to 21/02	12 days and 23 hours
2	From 22/03 to 29/03	6 days and 17 hours
3	From 29/03	Still in “primed conditons”

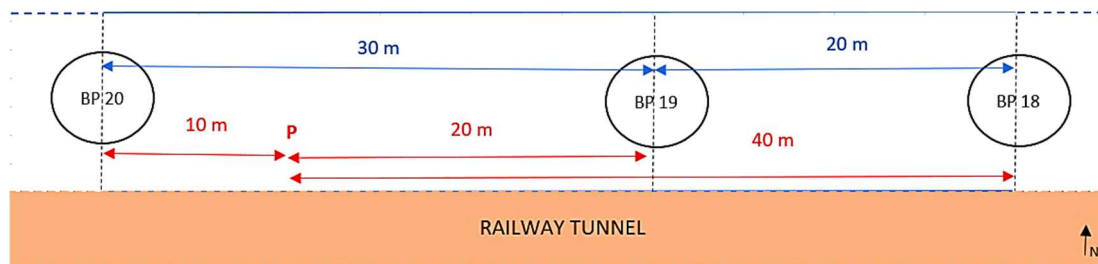


**Figure 33** Schematic representation of drainage trench

Figure 33 outlines a simplified schematic representation of how bypasses are spaced along the longitudinal direction whether in the upstream part or downstream. Considering at a given time a generic point P, total lowering in this point will be given by the sum of the lowering due to pumping test in bypass 20, plus the lowering due to pumping test in bypass 19 and the same for bypass 18, all of them considered at the same time.

In the estimation of lowering, as well as for increasing, boundary conditions presented in equations 5.4 and 5.5 were applied. The presence of the railway tunnel could not be nevertheless neglected: this represents a geohydrologic boundary that limit the continuity of the aquifer, invalidating one of the conditions for using the Theis equation. In particularly, the effect of a barrier boundary is to increase the drawdown in the wells and therefore to modify the hydraulic gradient, distorting cones of depression and affecting the time-rate of drawdown (Figure 34). In order to overcome that problem, the image-well theory is generally applied in these cases. The theory, introduced by Ferris (1959), states that “the effect of a barrier boundary on the drawdown in a well, as a result of pumping from another well, is the same as though the

aquifer were infinite and a like discharging well were located across the real boundary on a perpendicular way and at the same distance from the boundary as the real pumping well” [25]. In this way, the barrier boundary is replaced by imaginary wells which produce the same “disturbing effect” as the boundaries and the problem is solved considering an infinite aquifer where real and image wells operate simultaneously.

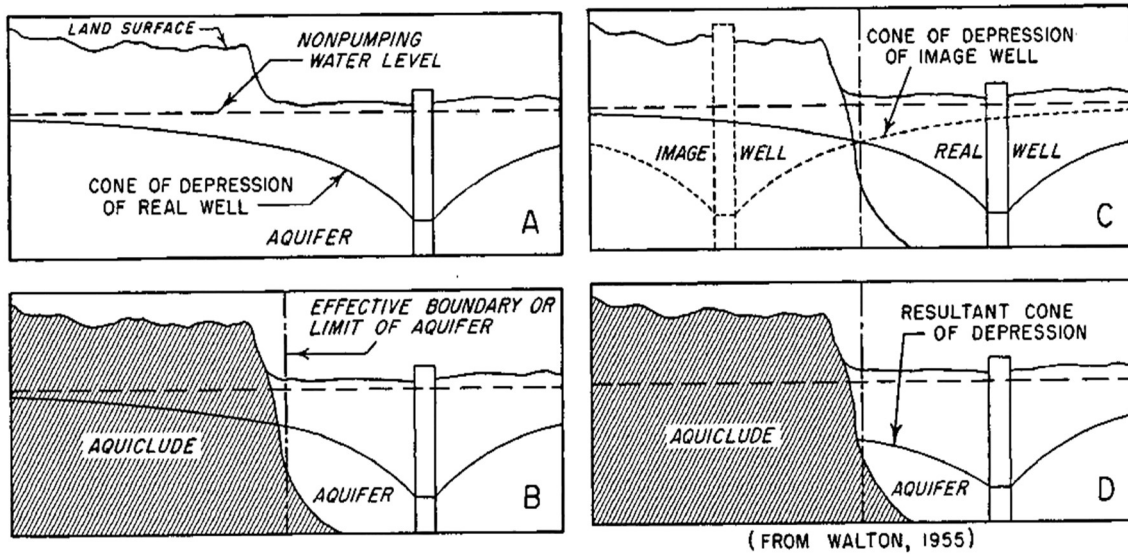


Figure 34 Schematic representation of the image-well theory in the case of a barrier boundary (Source [25])

The resultant real cone of depression will be therefore the sum of the components of both the real and image well depression cones as shown in Figure 34. In analytic terms, Eq. (5.9) will become:

$$s(r_r, t) = \frac{Q}{4\pi T} [W(u_r) + W(u_i)] \quad (5.13)$$

With:

$$u_r = \frac{Sr_r^2}{4Tt} \text{ and } u_i = \frac{Sr_i^2}{4Tt}$$

Where:  $r_r$  is the distance from the real well,  $r_i$  is the distance from the image-well.

For that specific case, siphons are placed at a distance of 0.75 meters from the slurry walls of the railway tunnel. Since, the response of the drainage trench is assessed through the line that links the three siphons, a distance of 1.5 meters was considered for the application of the image-well theory.

For a more correct interpretation of pumping tests, the different value of permeability that characterize the real aquifer beyond the drainage trench should be considered. This issue will be now neglected, considering very simplified conditions. It will be taken into account in Chapter 6.

Summarizing, starting from bypass 20 to bypass 18 and assessing the measurements every one meter, the following steps were performed:

1. At a given point, identification of longitudinal coordinates ( $r_{20}$ ,  $r_{19}$ ,  $r_{18}$ );
2. Estimation of  $u(r_{20})$ ,  $u(r_{19})$ ,  $u(r_{18})$  in real and image wells;

- 
3. Sum of the lowering/rising estimation coming from each siphon (with Jacob equation if  $u \leq 0.02$ , Theis equation if  $u \geq 0.02$ );
  4. Assess of the further decrease/rise of piezometric level due to the presence of railway tunnel with the image-well theory;
  5. Repeating from point 2 to 4 for each considered time;
  6. Total lowering/rising estimation.

### 5.3 Results and Discussion

Results globally showed a positive response of the drainage trench, allowing to decrease, especially in the first two pumping tests, the water levels of 0.26 meters in the upstream area close to the wells and of around 0.20 meters along the drainage trench. In this way, the difference of piezometric levels decreases around 0.40 meters, making therefore decrease, in the drainage trench area, the hydraulic gradient and consequently the “barrier effect” created by the railway tunnel.

How it was expected, with these conditions results were quite positive: drainage trench is an artificial structure built properly with the aim of increasing the ray of influence of the siphons and therefore increase their efficiency. It's hence characterized by hydrodynamic parameters that support the gravitational waterflow in the direction of the pumping wells. In fact, in the subsoil, solid particles are characterized by the presence of different types of water: hygroscopic water, pellicular water, gravitational water (A. F. Lebedev classification). The only type of water that can be mobilized is the gravitational water, i.e. the water that is not exposed to the action of the attraction forces toward the surface of the solid particles [29].

Going more in the detail, it also emerged from the results that variations of water levels are highly influenced by the presence of precipitations. Second pumping test started with same water levels of the first one and same ranges of flow rates were registered. At the end, results displayed same water levels decrease of the first one, taking however the half of its time to obtain the same values. Checking the weather conditions of February 2019, period in which the first pumping test was conducted, intense precipitations occurred in that period (Figure 35).

Finally, for the considered pumping tests, values of permeability around 0.17 m/s were obtained in the drainage trench. Since this is an artificial structure, these results were in line with the expectations.

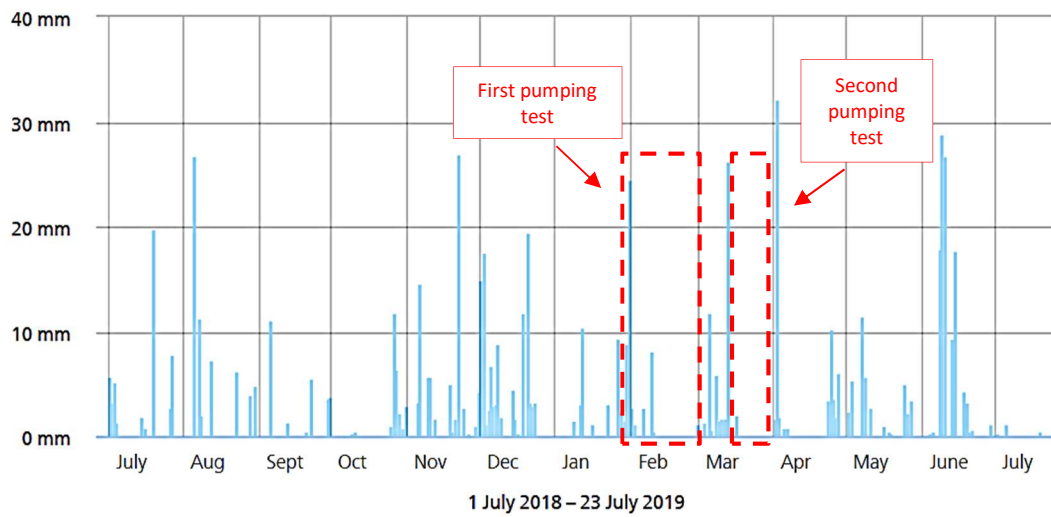


**Figure 35** Precipitation values recorded at Geneva Cointrin meteo station (Source MeteoSwiss)



**Figure 36** Schematic representation of lowering in the drainage trench obtained from the first pumping test

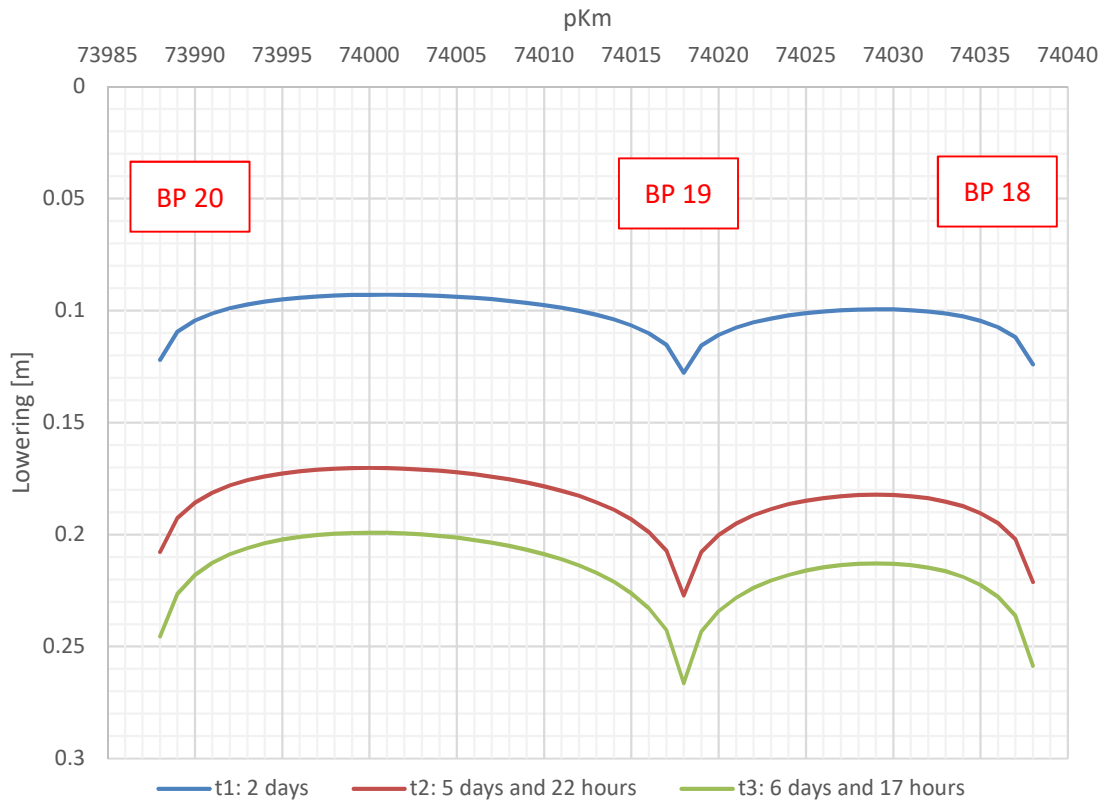


**Figure 37** Schematic representation of lowering in the drainage trench obtained from the second pumping test

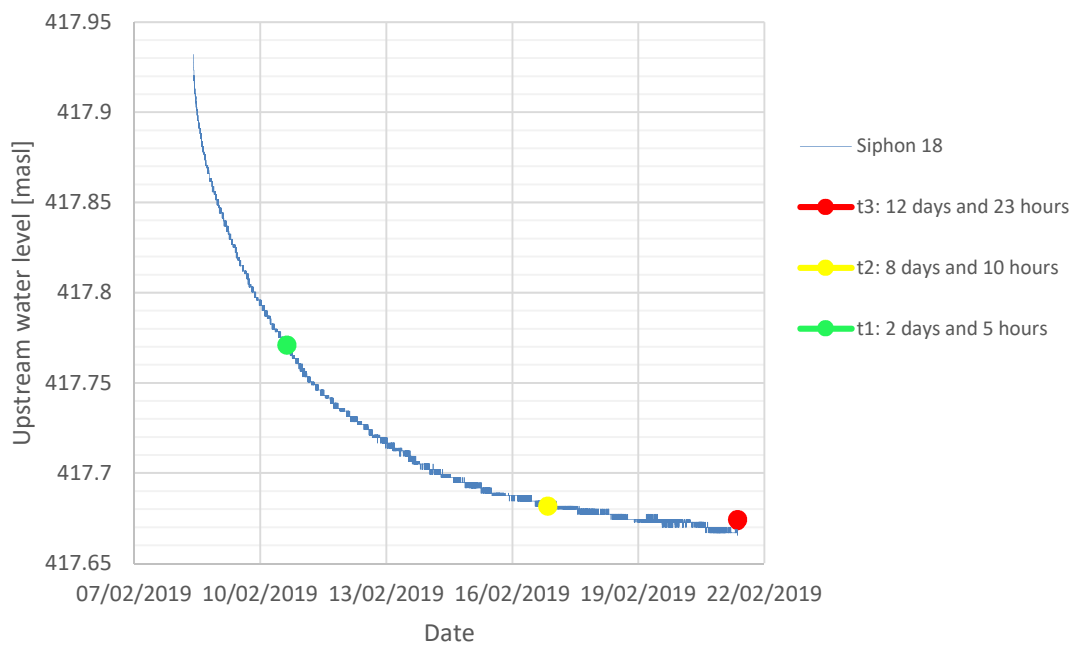


**Figure 38** Lowering registered in the upstream part of siphon 18 during the first pumping test for three different times

---

## Chapter 6. Analytical study of the aquifer

### 6.1 *Differences between drainage trench and aquifer*

The estimated response of the groundwater obtained in the drainage trench was found to be good as it was expected. Being an artificial structure, drainage trench is characterized by well-known properties: it's constituted by gravel, a material with high permeability ( $\sim 10^{-2}$  m/s) that facilitate the mobilization of the gravitational water located in the subsoil.

Beyond the drainage trench, the aquifer has different properties which can be mostly known through in situ tests such as geological surveys and multiple aquifer pumping tests. Geological surveys allow to analyze subsoil in depth, understanding its stratigraphy in that specific point and therefore the materials of which is formed. Basing on the type of material, these tests allow to have an idea of their degree of permeability. More reliable data can be obtained by multiple aquifer pumping tests which allow to better investigate the main hydrodynamic parameters: hydraulic conductivity and transmissivity. The more data are available, the more realistic the considered aquifer will be.

By considering all the hydrogeological information available on the webpage SITG (Système d'information du territoire à Genève), and tests conducted for CEVA project, presented in Chapter 3, the response of the aquifer was assessed. In particular, the aim was to investigate on how the aquifer is reacting beyond the drainage trench and to evaluate the distance up to which the groundwater is influenced by the pumping tests conducted into the siphon wells.

If in the drainage trench, being an artificial structure, parameters were more easily predicted, here the study was subjected to more hypothesis and uncertainties.

### 6.2 *Estimation of groundwater levels evolution*

In order to apply theory of pumping tests and therefore to evaluate the response of the aquifer, some simplifications were needed. In particular, uniform, homogeneous, isotropic conditions were considered. From the available data, it's known that Puplinge aquifer has in the investigated zone an average thickness of 5 meters and it's mainly constituted by gravel and sand. The only multiple pumping tests, for the estimation of the hydraulic parameters, were conducted during summer 2015, when the aquifer was characterized by low water table, and thus underestimated values of permeability were obtained. The considered values of hydraulic parameters used in this study were therefore computed taking more into account some preliminary estimations conducted in 2014 and considering also the piezometric tests available in that area.

Knowing the uncertainties to which results are subjected, and despite of the big simplification of the hydrogeological context, this study was useful for having an idea of the response of the aquifer at big scale. In Table 11, the main hydraulic characteristics are shown.

In particular, basing on the available hydrogeological data, the equivalent hydraulic conductivity was obtained by considering a gravel layer of 1 meter and a gravely-sand layer of 4 meters, an applying Eq.(6.1).

**Table 11** Main characteristics of the aquifer

Mean thickness of permeable layer [m]	5
Equivalent hydraulic conductivity [m/s]	0.076
Transmissivity [m <sup>2</sup> /s]	0.38
Specific yield [-]	0.3

**Table 12** Estimated hydraulic conductivity of each layer of the aquifer

Material	Depth [m]	Permeability K [m/s]	Equivalent permeability K <sub>eq</sub> [m/s]
Gravel	1	0.14	0.076
Gravelly-sand	4	0.06	

$$K_{eq} = \frac{\sum_{i=1}^{i=n} k_n \cdot D_n}{\sum_{i=1}^{i=n} D_n} \quad (6.1)$$

The response of the aquifer was conducted by following the same criterion adopted for drainage trench. The study was performed for all the three main pumping tests conducted in siphon wells (Figure 31) and considering three different distances: 20, 30, 50 meters.

As for the drainage trench, in order that all the conditions of applicability of Theis equation were respected, every pumping test was divided in small time ranges, as small pumping tests were considered, so that values of outflow were the most constant possible. At a given time and at a specific distance from drainage trench, for each considered point, the total lowering was obtained by the sum of the contribution of lowering coming from each well, with distances changing for each point (superposition principle). At the end of each cycle, the obtained lowering was added to the one achieved previously with the different discharge. Same approach was used for the estimation of water rising in the downstream sector. Measures were estimated every one meter in the longitudinal direction.

Figure 39 outlines a schematic representation of how response of the aquifer was assessed, whether in the upstream part or downstream. Considering at a given time a generic point P, placed at a certain distance from the drainage trench, total lowering in that point was obtained by the sum of the lowering due to pumping test in bypass 20, plus the lowering due to pumping test in bypass 19 and the same for bypass 18, all of them considered at the same time.

The same boundary conditions adopted for the drainage trench were also considered here, as well as for the presence of the “barrier effect” created by the railway trench, applying the image-well theory (Chapter 5).

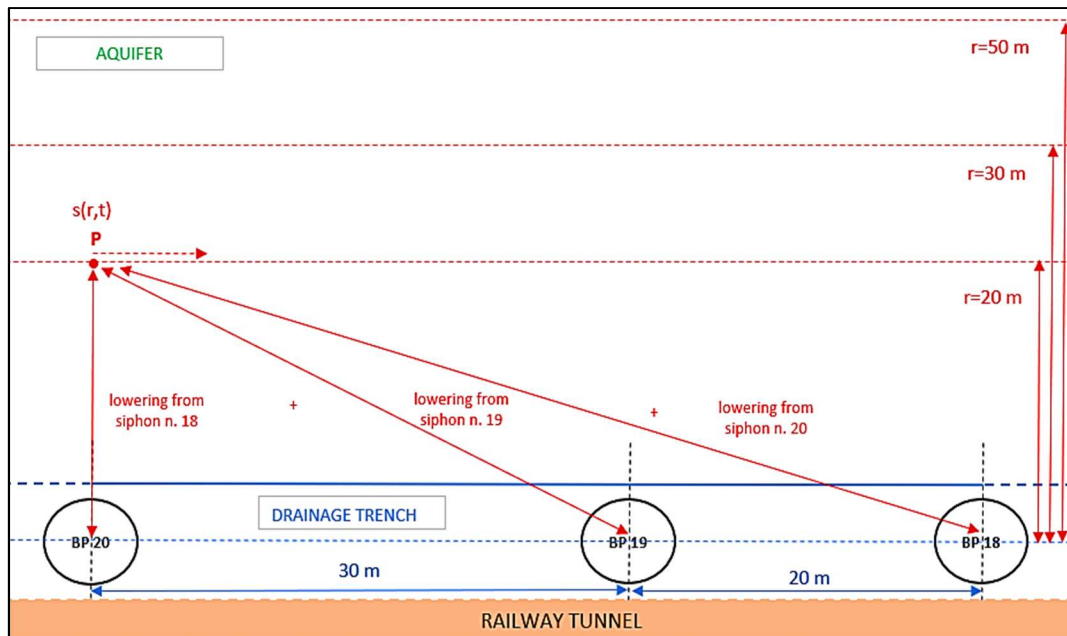


Figure 39 Schematic representation of aquifer

Summarizing, starting from bypass 20 to bypass 18, the following steps were performed:

1. At a given distance from drainage trench, identification of longitudinal coordinates ( $r_{20}$ ,  $r_{19}$ ,  $r_{18}$ );
2. Estimation of  $u(r_{20})$ ,  $u(r_{19})$ ,  $u(r_{18})$  in real and image wells;
3. At a given time period, so that discharge could be approximated to be constant, assessment of lowering (in the upstream part) and rising (in the downstream part), estimated for each point in the longitudinal direction (with Jacob equation if  $u \leq 0.02$ , with Theis equation if  $u \geq 0.02$ );
4. Assess of the further decrease/rise of piezometric level due to the presence of railway tunnel with the image-well theory;
5. Repeating from point 2 to 4 for each considered time, adding the results obtained in the previous time period with the achieved new one;
6. Total lowering/rising estimation.

### 6.3 Results and Discussion

As for the drainage trench, results of the first two pumping tests showed each other a similar behavior. Since the same range of discharge was recorded in the two pumping tests, a similar lowering was obtained in the aquifer, despite the different duration of the two tests (Chapter 5.3). Considering the time corresponding to the end of the pumping tests, at a distance of 20 meters from the drainage trench, a lowering of approximately 0.20 meters was assessed in the first pumping test and of around 0.18 meters in the second one. This result is very good considering that along the drainage trench a similar response was obtained. Increasing the distance from the drainage trench, as it is expected, the drawdown effect in the aquifer decreases. At a distance of 50 meters, a lowering of around 0.15 meters was estimated along all the longitudinal direction in both pumping tests. These results are showed in Figure 40 and

Figure 41, comparing the values obtained for the aquifer with the ones achieved in the drainage trench.

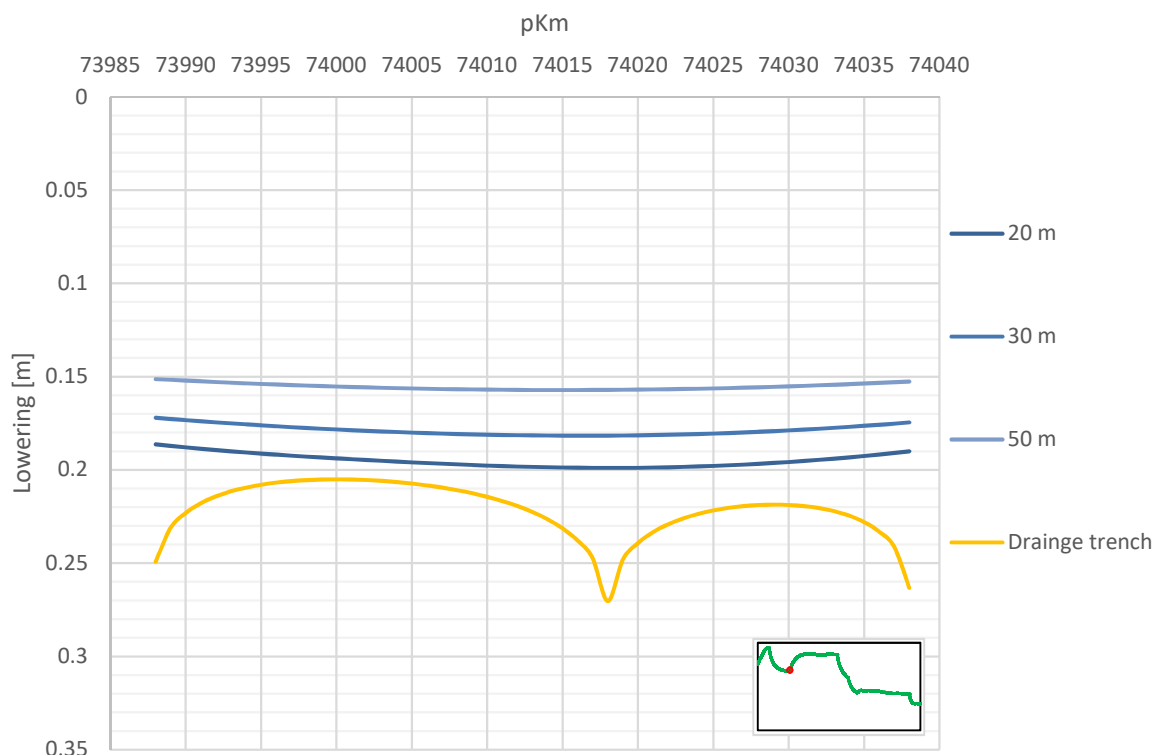
Third pumping test gave a lower response of the aquifer, due to the different range of discharges and the different considered times. In this last case, at a distance of 20 meters from the drainage trench, a lowering of around 0.14 was obtained, and at distance of 50 meters the response was approximately of 0.8 meters. These results are only referred to the pumping test conducted from 29<sup>th</sup> March. Therefore, the assessed lowering doesn't take into account the response of the aquifer obtained in the previous month.

The same responses were assessed in the downstream part of the aquifer, considering the three pumping tests at the three different distances. In this way, the increase of groundwater levels was evaluated in this section. Results are outlined in Appendix D.

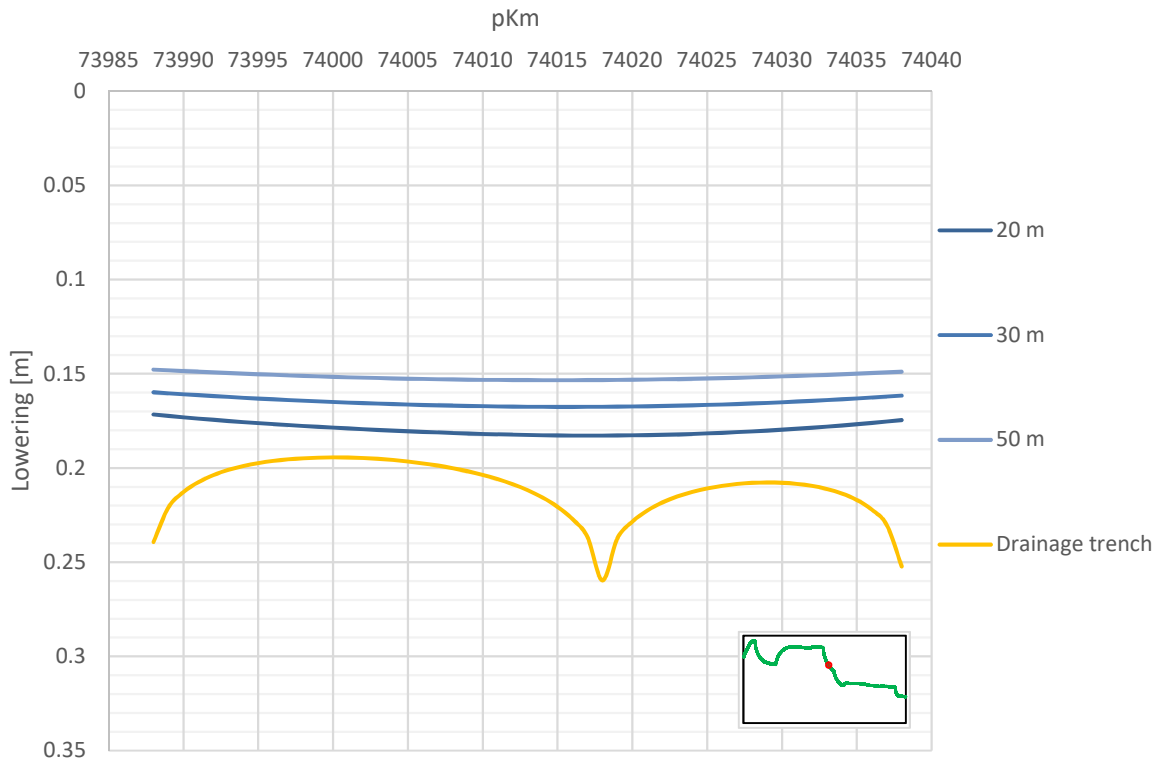
In Figure 40 and Figure 41, lowering of the aquifer assessed at a distance of 50 meters was compared, for the first two pumping tests, with one estimated in the drainage trench. How it can be seen, the two responses are characterized by the same behavior, following the same trendline.

Figure 42 and Figure 43 show the evolution in time of the lowering assessed in siphon n.19, in the upstream well and in the aquifer at a distance of 50 meters, both in the first and second pumping test.

Globally, it could be therefore affirmed that, in these simplified conditions, and with the adopted hydrogeological parameters, the aquifer has a good response and is reacting well to siphons operation.



**Figure 40** Lowering estimation of the aquifer during first pumping test



**Figure 41** Lowering estimation of the aquifer during second pump test

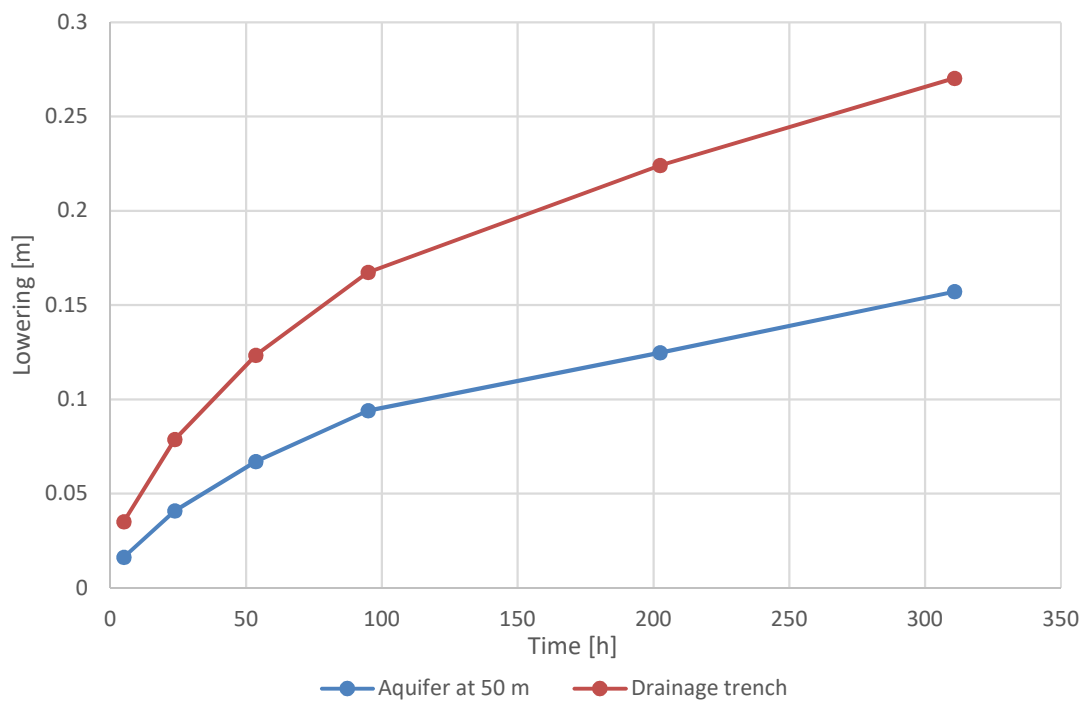


**Figure 42** Evolution in time of lowering in siphon 19 and in the aquifer at 50 meters during first pumping test

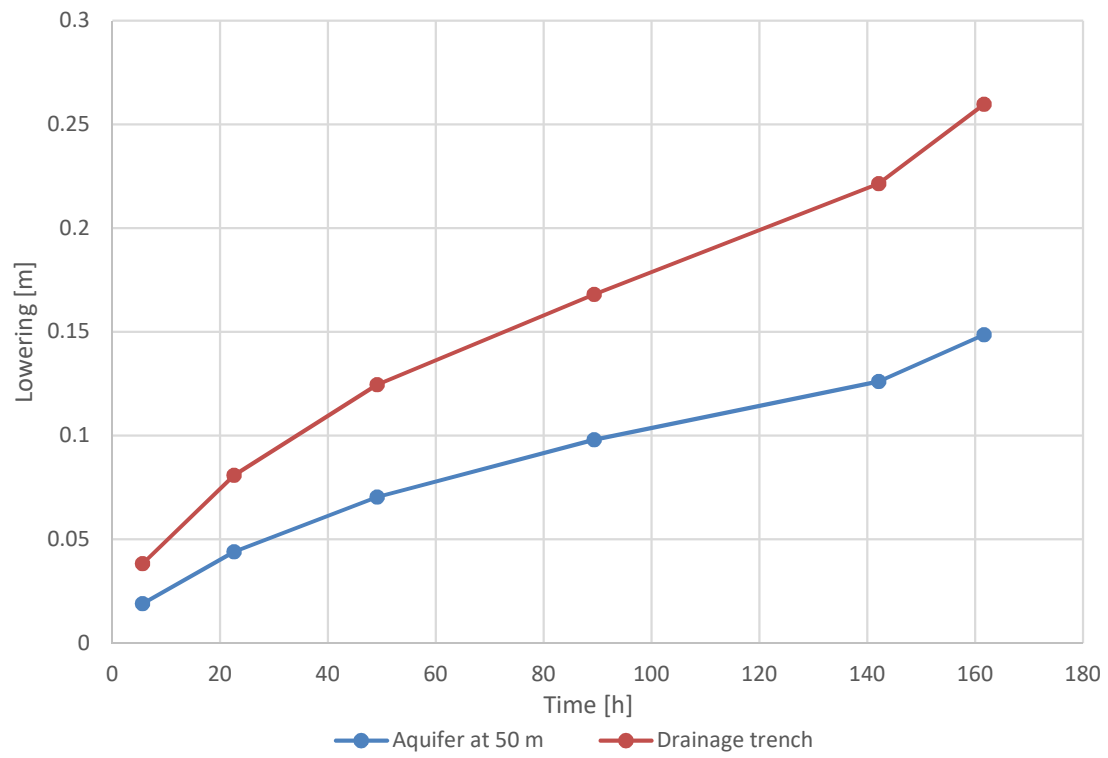


**Figure 43** Evolution in time of lowering in siphon 19 and in the aquifer at 50 meters during second pumping test

---

# Chapter 7. Conclusions

## 7.1 *Final discussion*

To summarize, this work was essentially based on the evaluation of how Pupliche aquifer is reacting to the siphons functioning and if the two aquifer sections, upstream and downstream part, are slowly reconnecting.

In particular, the study was focused on siphons 18, 19 and 20, i.e. siphons that are better connected. In fact, monitoring the water levels in both wells of each siphons, the three ones chosen for this study are the ones that show a better response, with water levels characterized by similar trends either in upstream or in downstream part.

Studies were performed as follows.

Firstly, discharge into the three siphon systems was estimated. This part was essentially developed starting from the experimental studies conducted on the physical model in 2017. By means of Darcy-Weisbach equation, water level-discharge relationship was firstly estimated in the physical model and then in siphons in field.

The estimation of the flow rate was fundamental for the assessment of the response of the aquifer. This latter was firstly studied along the drainage trench and then in the real aquifer, at different distances from the siphons.

Drainage trench is an artificial system built from siphons 18 to 24 in order to increase the efficiency of capture and release of water respectively in the upstream and downstream sector. Since it is made of gravel (high permeability), it supports the gravitational waterflow in the direction of the pumping wells. Here studies were performed basing on Theis theory. The goal was to assess water levels lowering in the upstream area as well as the increase of water levels in the downstream part. Open boundary conditions were considered on the left and on the right of siphons, as well as in north and in south part. The presence of the railway tunnel, which is an impermeable limit, was counted by using the image-well theory. Hydrodynamic parameters, in particular permeability and transmissivity, were defined considering aquifer pumping tests as well as piezometric data collected in the previous years.

Same approach was adopted for the estimation of the response of the aquifer at different distances from the drainage trench. In particular, assessments were conducted at distances of 20, 30 and 50 meters from the drainage trench, in upstream and downstream part. An aquifer with simplified hydrogeological characteristics was considered, in particularly with uniform, homogeneous and isotropic conditions. Lowering in the upstream part, as well as rises in the downstream part were assessed, for the different distances, every one meter along the longitudinal direction.

From the analytical studies conducted in these months, it can be asserted that, since February 2019, drainage trench as well as the aquifer have been demonstrating a good reaction at the functioning of siphons 18, 19, 20, both in upstream and downstream part.

As it was predicted during the preliminary studies conducted in 2015 [19], the realization of the drainage trench was essential for achieving the capture and release of water respectively in the upstream and downstream sector.

From February to July 2019, as it is showed in Table 13 and Table 14, water levels into upstream siphons wells decreased of around 0.40 meters, as well as on the downstream wells, where they increased of the same amount. This means that in approximately 8 months, difference of water levels between the two sector ( $\Delta H$ ) decreased of around 0.80 meters. The evolution of water levels in the three siphons, during these months, is outlined in Figure 44, both for upstream and downstream sector.

Along the drainage trench, considering pumping test 2 (Chapter 5.3) and pumping test 3 (Appendix C.3), a lowering of approximately 0.32 meters was estimated between bypass 20 and 19 in the upstream part and a similar value of water rising was registered in the downstream section, thus producing an overall decrease of difference of water level ( $\Delta H$ ) on the drainage trench of around 0.60 meters.

In the same period, at a distance of 50 meters from the siphons wells, aquifer registered a decreased of water levels in the upstream part of approximately 0.24 meters ( Figure 41 and Appendix D.3). These results, also confirmed by the presence of piezometer 718, represented a positive outcome, generating a decrease of the difference of water levels between the two sector ( $\Delta H$ ) of approximately 0.50 meters.

**Table 13** Total water variation registered in siphon wells from February to July 2019

	<b>Wells</b>		
	BP 18	BP 19	BP 20
<i>Upstream decrease [m]</i>	0.40	0.40	0.40
<i>Downstream increase [m]</i>	0.40	0.40	0.41

**Table 14** Total lowering registered in the aquifer at a distance of 50 m from February to July 2019

	<b>Aquifer</b>		
	BP 18	BP 19	BP 20
<i>Upstream decrease [m]</i>	0.241	0.250	0.239

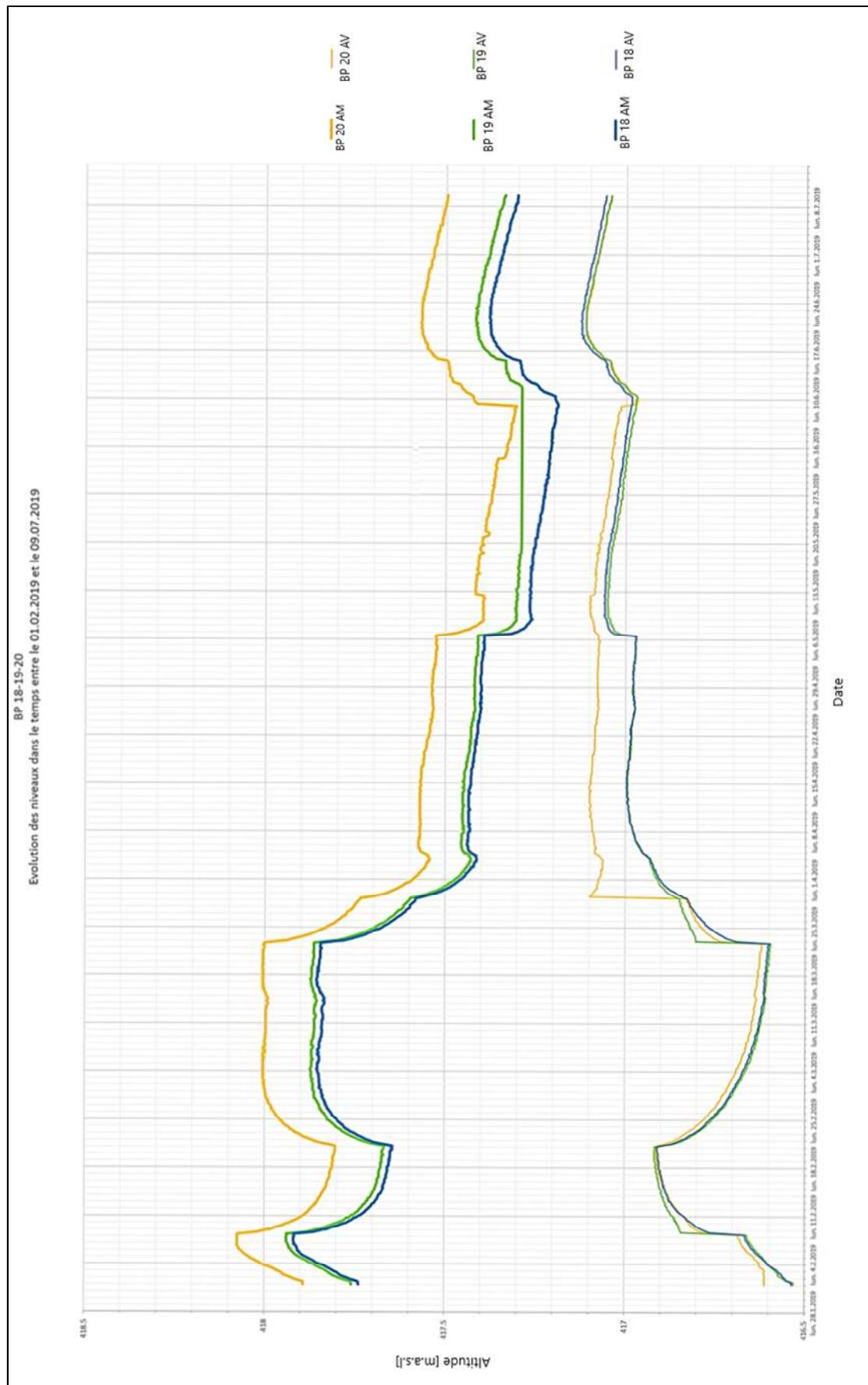


**Figure 44** Evolution of water levels in the three siphons from February to July 2019 (Source BG)

If siphons 18, 19, 20 are functioning in the right way making decrease the hydraulic gradient and slowly reconnecting the sections of the aquifer, a more complex state is registered in the other five siphons.

Since February 2019, siphon 21 is unstable, with high difference of water levels between upstream and downstream (Figure 45).

Siphons 23, 24 and 25, since the beginning, have been recording water levels that are higher in the downstream part. This behavior is related, with high probability, to the complexity of the geology in that area. For these reasons, these siphons are not in operation (Figure 45, Figure 46).

Finally, since 21.02.2019, siphon 26 is working with regular intermittence (fluctuating aquifer).

Despite the complex working conditions of these last siphons, it can be asserted that, considering the groundwater in its complexity and taking also into account the contribution given by Foron river with its partial evacuation of water, Puplinge aquifer is reacting well.

For estimating the response of the aquifer, the analytical approach was a useful method that, despite the required simplifications both for the drainage trench model and for the real aquifer model, allowed to understand the behavior of the entire aquifer-siphon system.

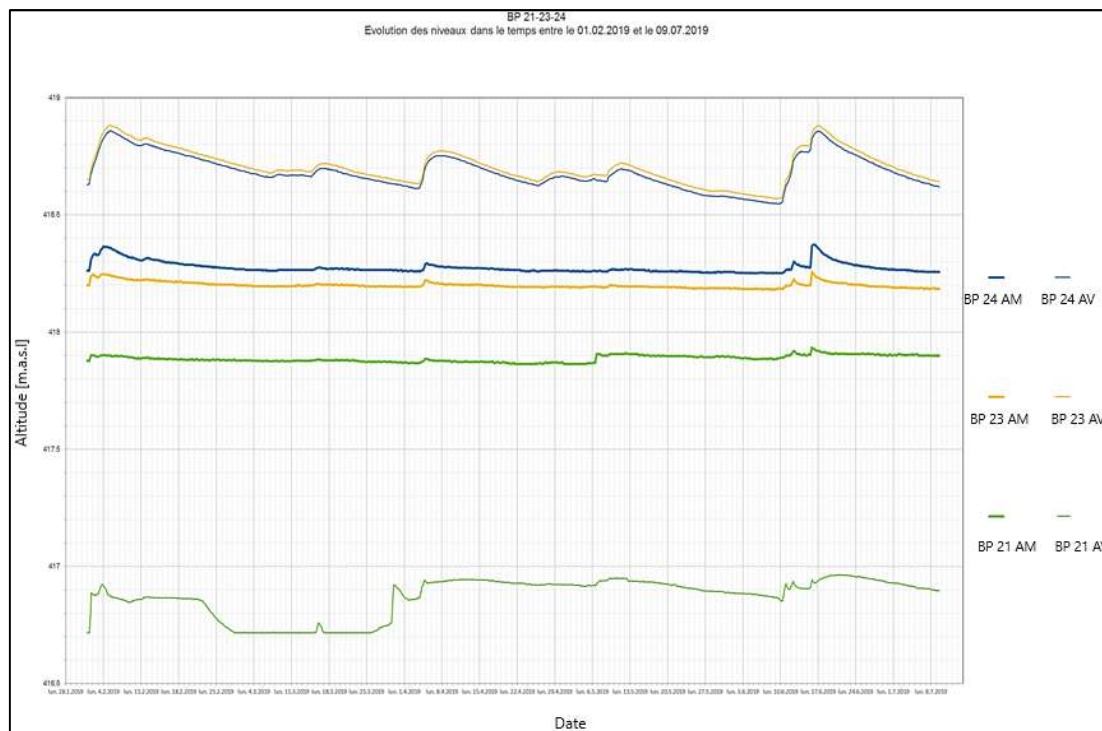
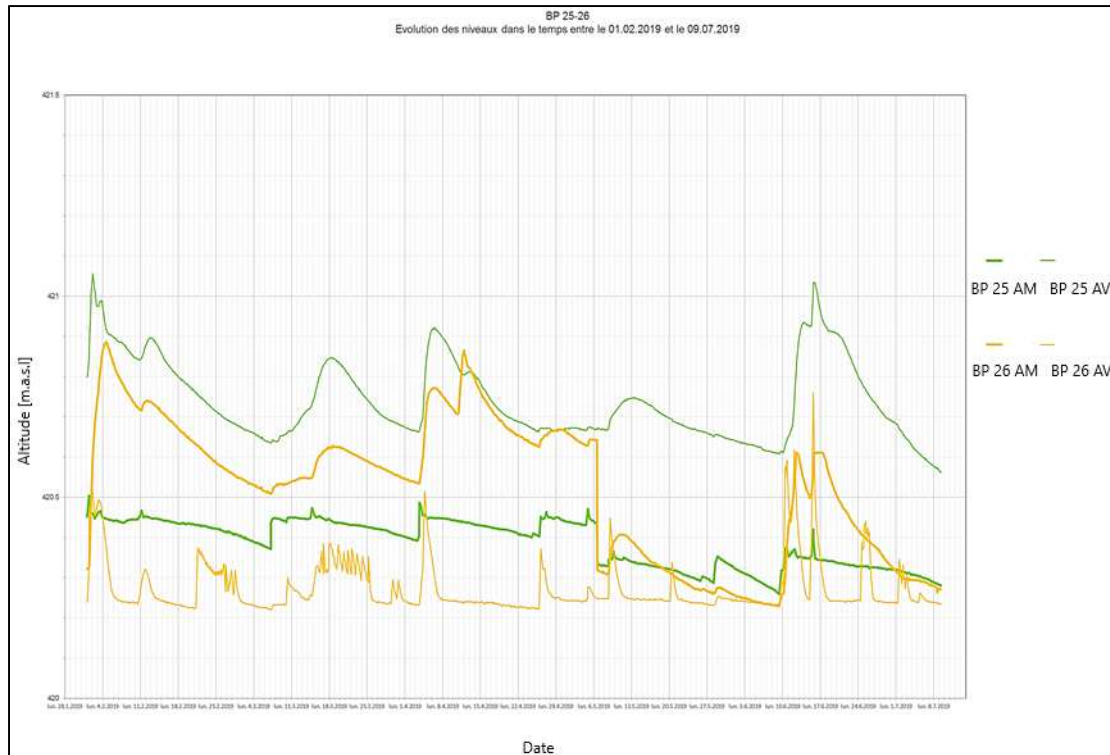


Figure 45 Response of siphons 21-23-24 (Source BG)



**Figure 46** Response of siphons 25-26 (Source BG)

## 7.2 Future work

Considering that the flow rate into the siphons, estimated in an analytical way, was at the base of the assessment of the aquifer response, it would be convenient to estimate discharges with a second method, in order to compare the two results and to verify the validity of the adopted analytical approach.

The idea of installing a flowmeter on field was strongly considered, and on 29<sup>th</sup> July, a portable ultrasonic clamp-on flowmeter was installed on field in siphon 19.

This instrument will represent an important help for the project, and it is essentially based on transmitting and receiving acoustic signals along a diagonal measuring path. In particular, sound wave going downstream with the flow travels faster than a sound wave going upstream against the flow. The difference in transit time is directly proportional to the mean flow velocity of the medium.

The instrument was firstly calibrated at Laboratory of Hydraulic Construction, where tests at different discharges were conducted and it was assessed that it has a percentage of error lower than 4%.

In order to make it work in the best way, it was installed on field in the upstream part of the siphon, avoiding the highest points (risk for air bubbles). In fact, the presence of air is not able to give proper measurements. With high probability, in this case, the quality of the signal of the instrument would be very low, recording very unstable values.

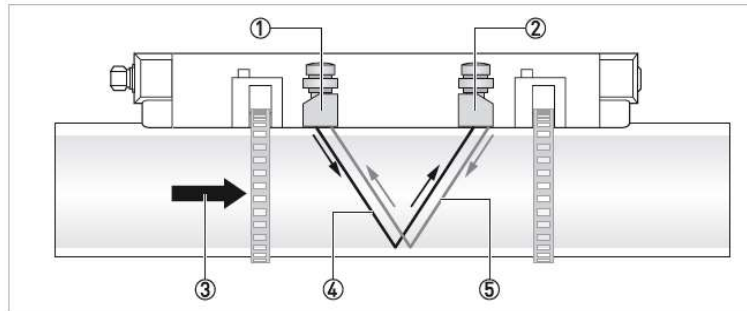


**Figure 8-1: Measuring principle**

- ① Transducer A
- ② Transducer B
- ③ Flow velocity
- ④ Transit time from transducer A to B
- ⑤ Transit time from transducer B to A

**Figure 47 - Measuring principles (Source: Handbook OPTISONIC 6300 P)**

Optisonic flowmeter has an autonomy of around 14 hours. Since the idea was to register values of flow rate for at least 10 days, it was necessary to install on field an additional external battery (Figure 48). When first measurements will be available, it will be possible to compare these data with the values estimated in the analytical way. It will be therefore possible to compare the two methods and finally have a realistic value of the discharge that flows into the system.

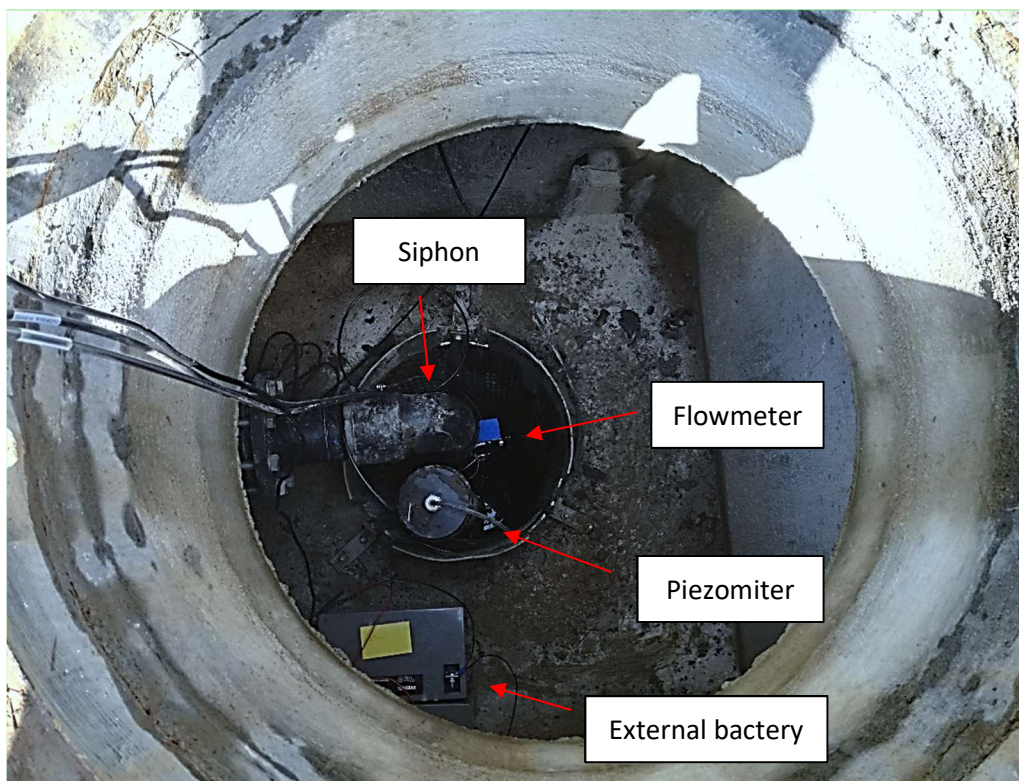


**Figure 48 Siphon 19 with the installed flow meter**

---

The installation of the flowmeter will be also useful for a better estimation of how discharge changes by artificially increasing the difference of water levels between upstream and downstream.

In particular, discharge in siphon 19 could be firstly assessed when all the three siphons are in working conditions.

Afterwards, the increase of upstream water levels as well as discharge in siphon n.19 could be assessed by firstly closing bypass 18, and then also siphon 20.

Finally, setting siphons 18 and 20 in prime condition, flow rate in siphon n.19 could be monitored again, comparing results with the ones obtained previously.



# Appendix A – Additional equations

## A.1. Atmospheric pressure

$$h = \frac{P_{atm}}{\rho_{H2O} \cdot g} = \frac{101325 \text{ Pa}}{1000 \text{ kg/m}^3 \cdot 9.81 \text{ m/s}^2} \cong 10.33 \text{ m}$$

## A.2. Henry's law

$$C = K \cdot P$$

Where:

C: concentration of the gas in the solution [mol/l];

k: constant of the considered gas [mol/atm·l];

P: gas pressure [atm].

## A.3 Weir equation

$$Q = 0.44\pi\sqrt{2gh^{1.5}}$$

## A.4 Vortex equation (Mulligan)

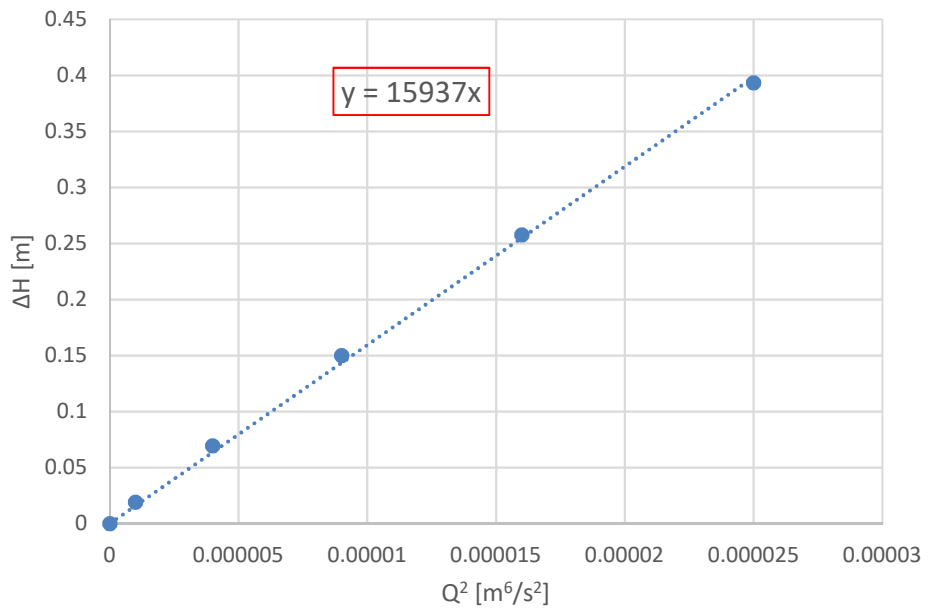
$$Q = \frac{k_\alpha}{\left(\frac{5\alpha d}{h}\right)^{n_\alpha}} \sqrt{g} d^{5/2}$$

## A.5 Head losses distribution considering the siphon system without vortex chamber

$\sum K_i = 1.43$  (local head losses at the entrance) + 2.8 (local head losses at the outlet) + 1.1·2 (90 degree miter bend in both corners) = 6.43

$$h_{loc} = \frac{16}{\pi^2 D^4} \frac{\sum k_i}{2g} Q^2 = 8097 \cdot Q^2$$

Q [l/s]	1	2	3	4	5
Re [-]	14147	28294	42441	56588	70736
f [-]	0.0283	0.024	0.0219	0.0205	0.0196
$h_f$ [m]	0.011	0.037	0.077	0.128	0.191
$h_{loc}$ [m]	0.008097	0.032388	0.072873	0.129552	0.202425
$\Delta H$ [m]	0.019097	0.069388	0.149873	0.257552	0.393425

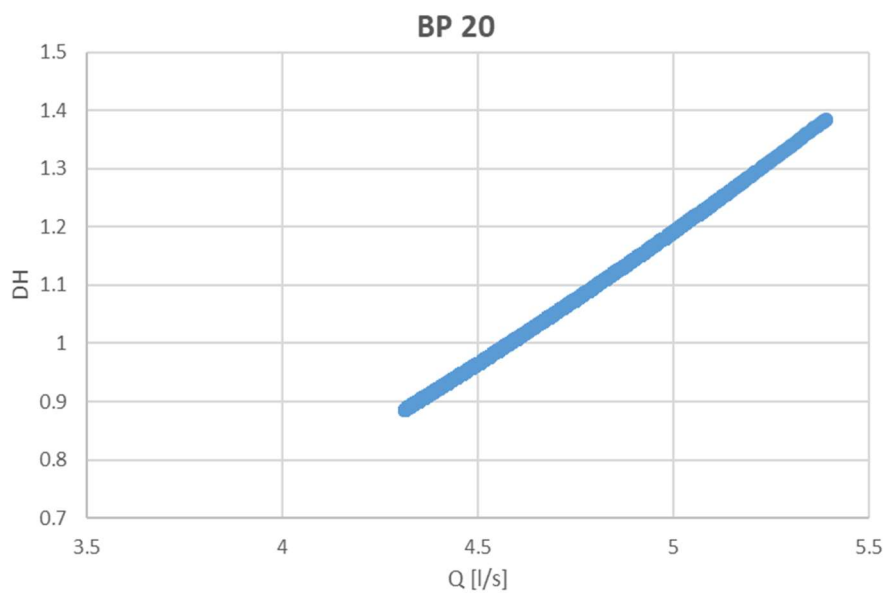
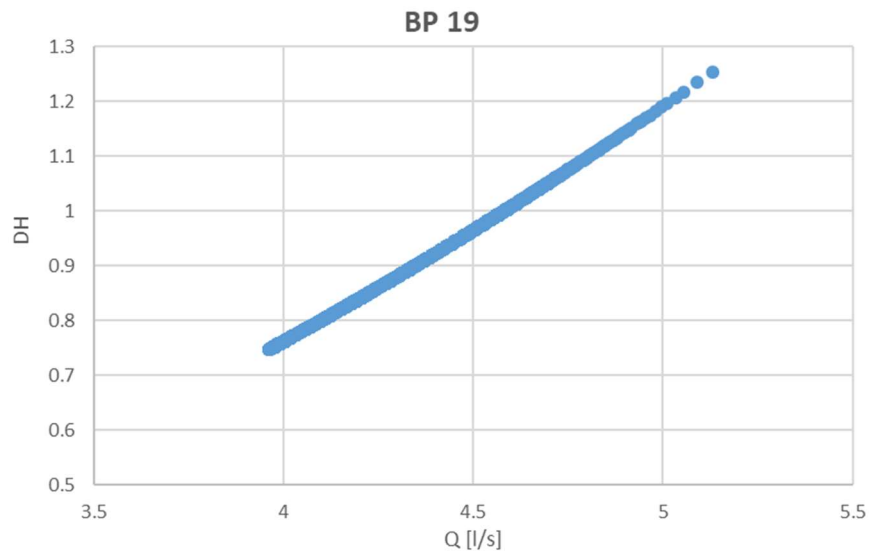


The graphic above represents the  $\Delta H$ - $Q$  relationship of the siphons without vortex chamber.

---

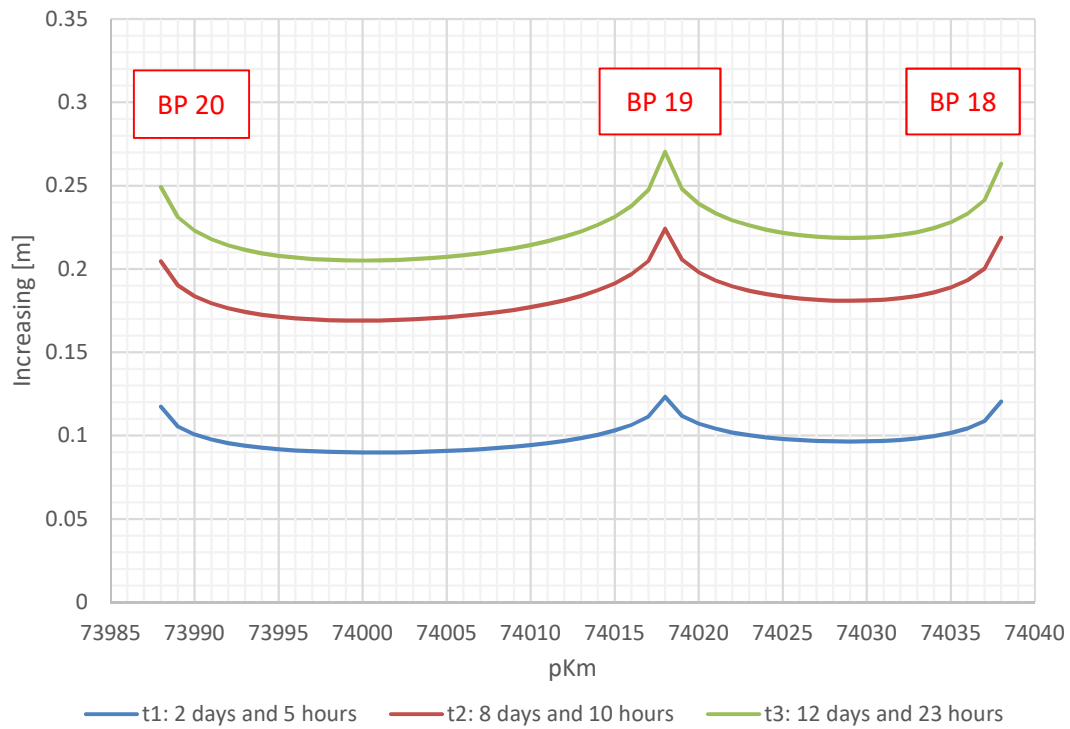
## Appendix B – Discharge during first pumping test

The followings graphics represent the range of discharge obtained in siphon n.19 and n.20 during pumping test conducted from 8.02.2019 to 21.02.2019. due to the high difference of water levels registered in this period, high values of flow rate were assessed.

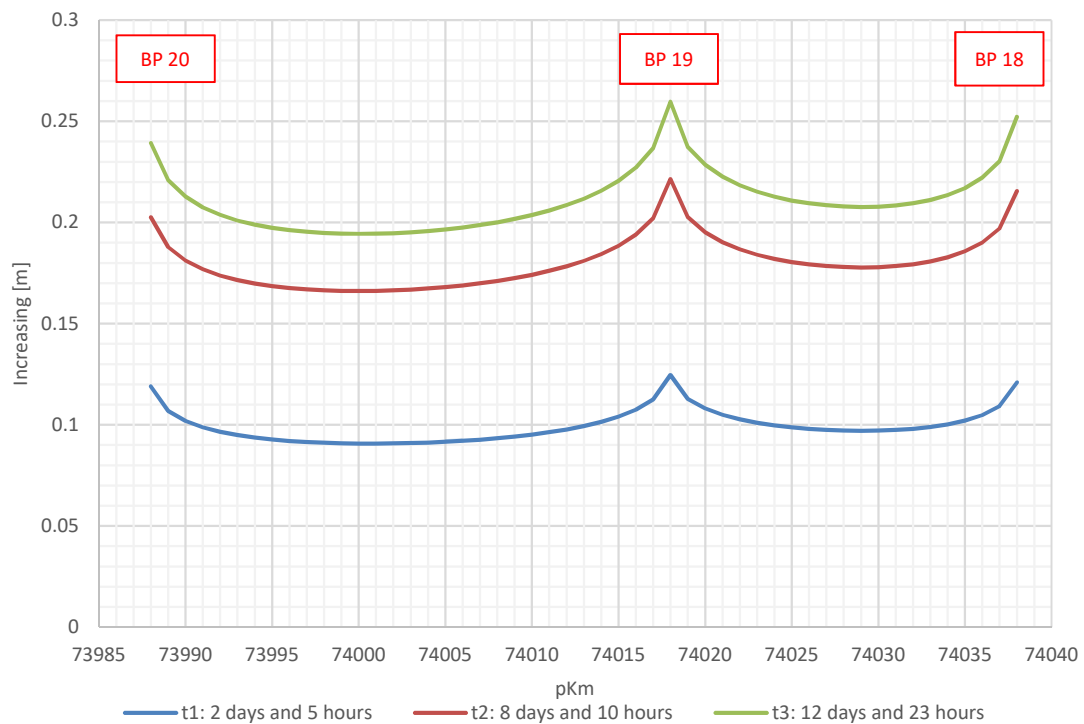


# Appendix C – Estimation of groundwater levels evolution in drainage trench

## C.1. Increasing of water level during first pumping test



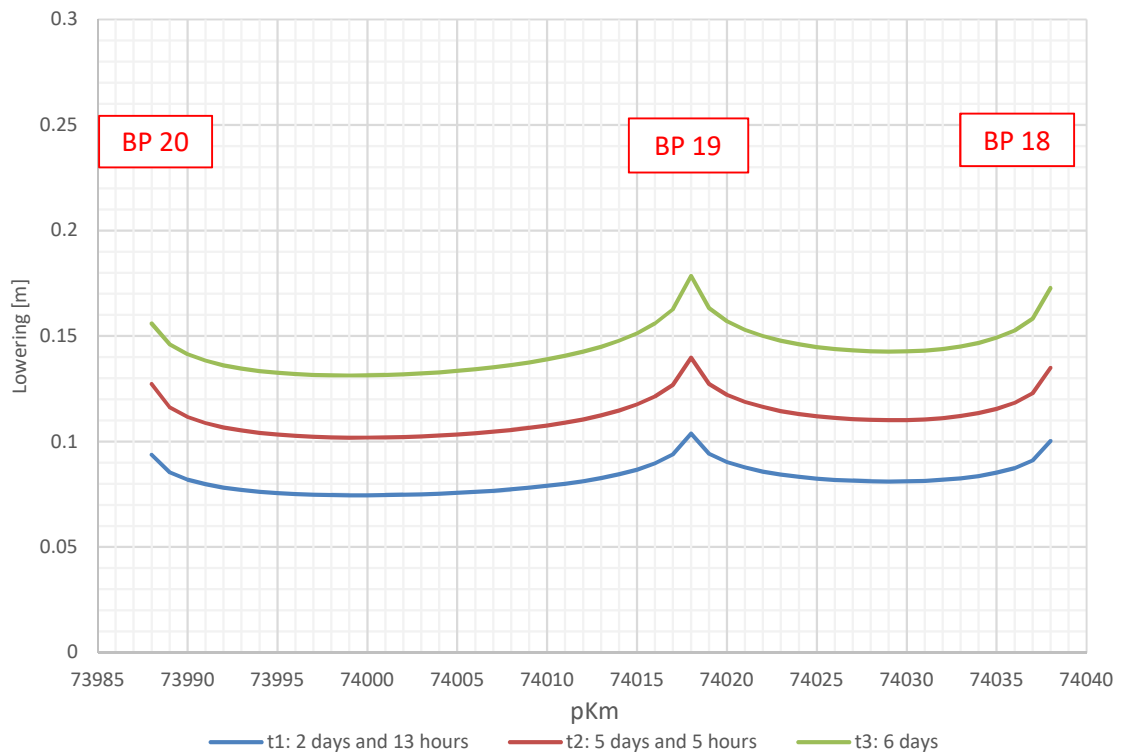
## C.2. Increasing of water level during first pumping test



### C.3. Lowering of water level during third pumping test

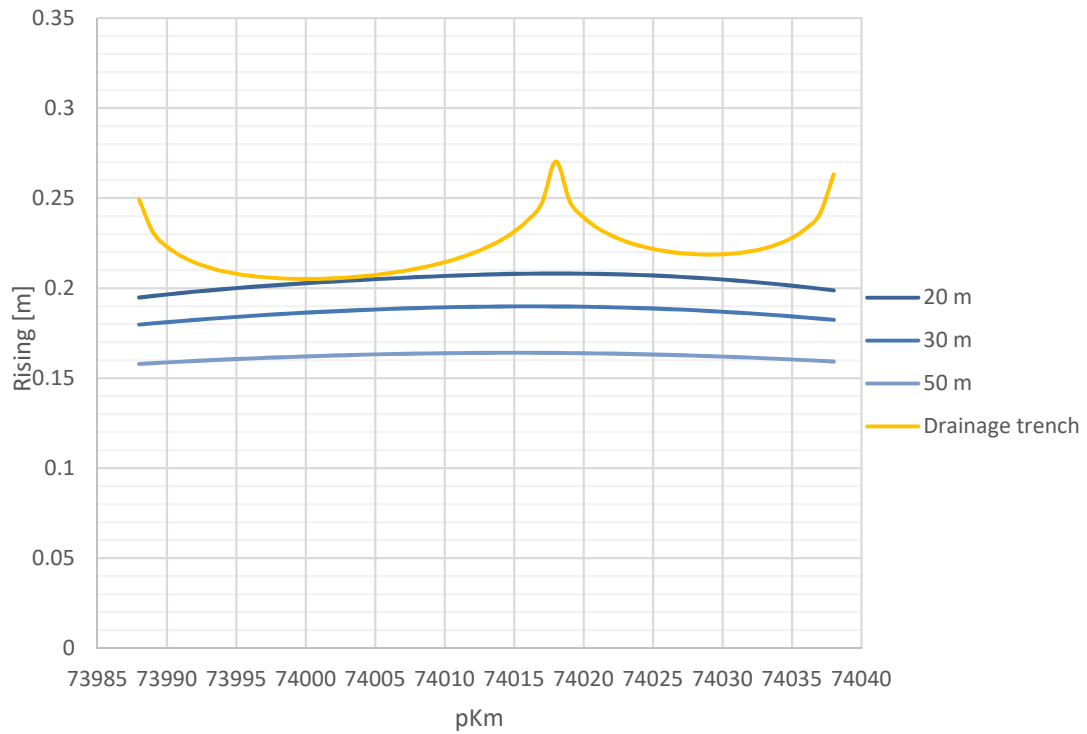


### C.4. Increasing of water level during third pumping test

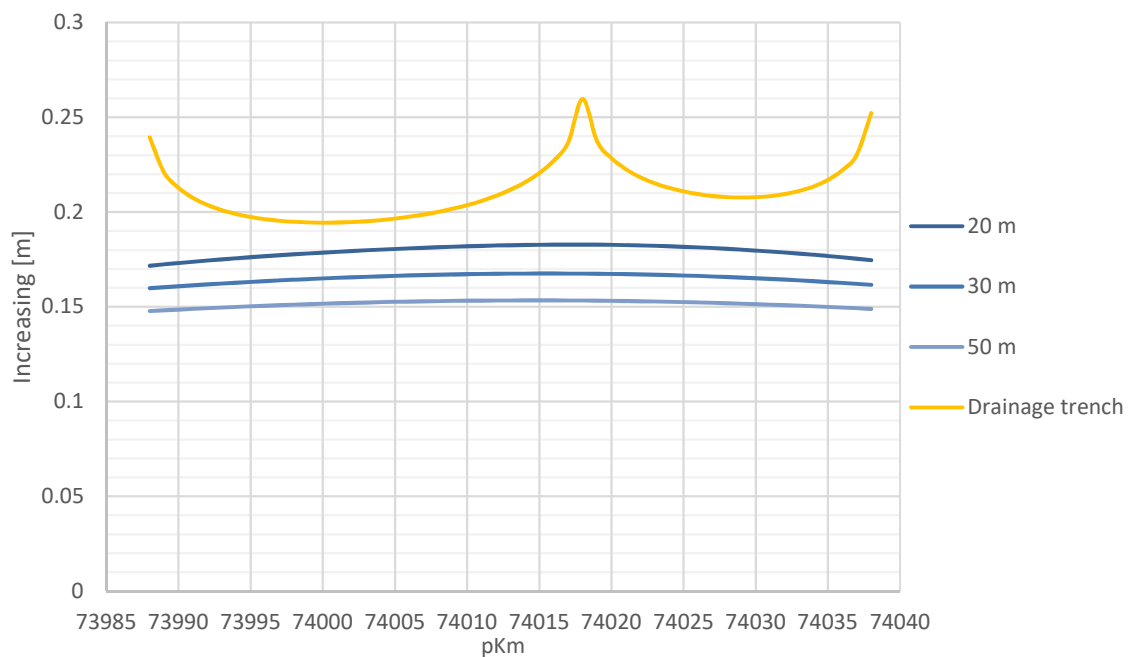


# Appendix D - Estimation of groundwater levels evolution in the aquifer

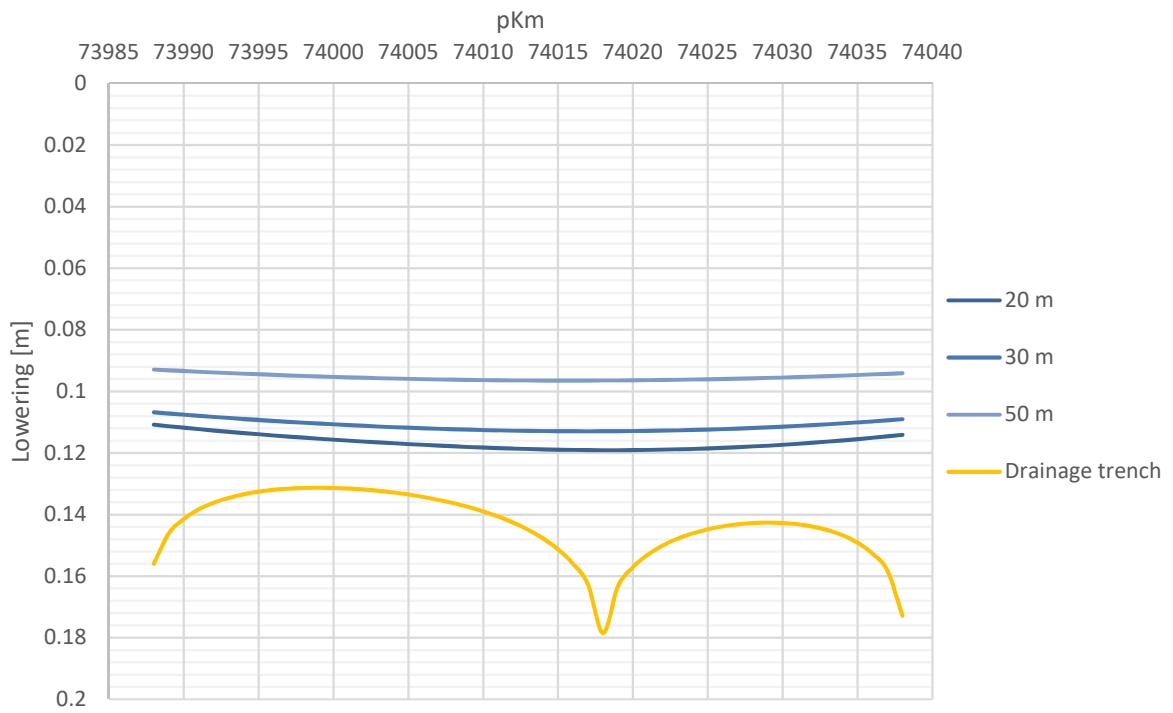
## D.1. Increasing of water level during first pumping test



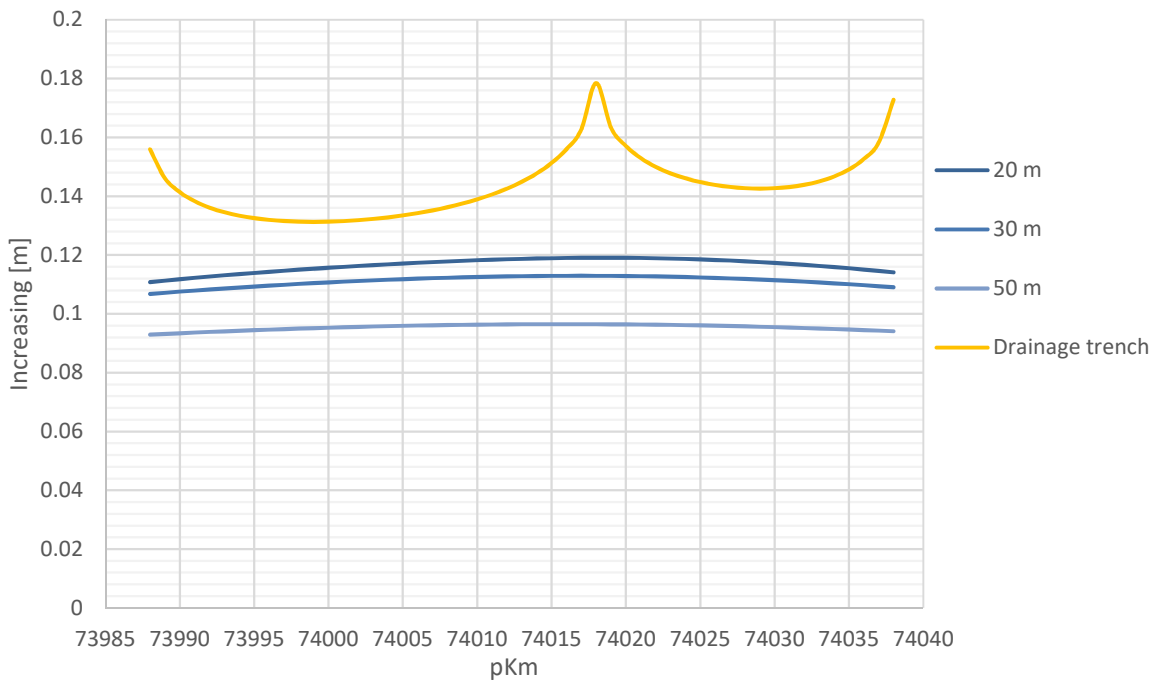
## D.2. Increasing of water level during second pumping test



### D.3. Lowering of water level during third pumping test



### D.4. Increasing of water level during third pumping test





---

## References

- [1] P. Marinos and M. Kavvas, 'Rise of the groundwater table when flow is obstructed by shallow tunnels', presented at the 37th Congress of the Int. Assoc. of Hydrogeologists on Groundwater in the Urban Environment, Nottingham, UK, 1997.
- [2] G. Attard, T. Winiarski, Y. Rossier, and L. Eisenlohr, 'Review: Impact of underground structures on the flow of urban groundwater', *Hydrogeol J*, vol. 24, no. 1, pp. 5–19, Feb. 2016.
- [3] 'CEVA en bref', *Projet CEVA*, 11-May-2017. [Online]. Available: <https://www.ceva.ch/2017/05/11/ceva-en-bref/>.
- [4] 'FAQ sur le projet', *Projet CEVA*, 15-Jun-2017. [Online]. Available: <https://www.ceva.ch/2017/06/15/a-propos-projet/>.
- [5] F. Geiser, 'Rapport concernant la charge OFT 2.26.6', Project CEVA, 2012.
- [6] A. Bragadir and S. Goy, 'BG - Rétablissement de l'écoulement de la nappe phréatique - project de by-pass', 2014.
- [7] 'Siphon', *Wikipedia*. 14-Apr-2019.
- [8] R. Salama, R. Ali, D. Pollock, J. Rutherford, and V. Baker, 'Review of Relief wells and siphons to reduce groundwater pressures and water levels in discharge areas to manage salinity', *A Report to Water & Rivers Commission, WA*, 2003.
- [9] Y. Cai, H. Sun, Y. Shang, and Z. Wu, 'Air accumulation in high-lift siphon hoses under the influence of air dissolution and diffusion', *J. Zhejiang Univ. Sci. A*, vol. 16, no. 9, pp. 760–768, Sep. 2015.
- [10] G. De Cesare, K. Essyad, P. Furlan, V. N. Khuong, and S. Mulligan, 'Experimental Study at Prototype Scale of a Self-priming Free-Surface Siphon', in *Advances in Hydroinformatics*, P. Gourbesville, J. Cunge, and G. Caignaert, Eds. Singapore: Springer Singapore, 2018.
- [11] M. Cellino and K. Essyad, 'Underground water production by siphons in the Bern (Switzerland) drinking water supply system', *International Conference on Computing and Control for the Water Industry CCWI 2001 - Leicester*, 2001.
- [12] W. H. Hager, 'Head-Discharge Relation for Vortex Shaft', *Journal of Hydraulic Engineering*, 1985.
- [13] S. Mulligan, 'Experimental and Numerical Analysis of Three-Dimensional Free-Surface Turbulent Vortex Flows with Strong Circulation', (Ph.D dissertation), IT Sligo, 2015.
- [14] J. Knauss, Ed., *Swirling Flow Problems at intakes*. Rotterdam: Balkema, 1987.
- [15] S. Mulligan, J. Casserly, and R. Sherlock, 'Effects of Geometry on Strong Free-Surface Vortices in Subcritical Approach Flows', *Journal of Hydraulic Engineering*, vol. 142, no. 11, 2016.
- [16] V. N. Khuong, 'CEVA SECTEUR 7 : ETUDE, PROJET ET SUIVI DE MISE EN OEUVRE DE BY-PASS AVEC SIPHON AUTO-AMORÇAN. RÉALISATION D'UN MODÈLE PHYSIQUE À L'EPFL - LCH', 2016.
- [17] V. N. Khuong and K. Essyad, 'CEVA SECTEUR 7 : ETUDE, PROJET ET SUIVI DE MISE EN OEUVRE DE BY-PASS AVEC SIPHON AUTO-AMORÇAN. ESSAIS SUR PROTOTYPE EN LABORATOIRE ET ESSAIS DE RÉCEPTION IN SITU'. 2017.
- [18] F. Geiser and J. Crisinel, 'CEVA LOT 7 - RAPPORT DE SYNTHÈSE SUR LES ETUDES DE LA NAPPE DE PUPLINGE', 2006.

- 
- [19] 'CEVA – Lot 37.20 – Essais de pompage sur bypass' .
- [20] A. Molfetta and R. Sethi, *Ingegneria degli acquiferi*. Milano: Springer Milan, 2012.
- [21] 'The Darcy-Weisbach Equation'. [Online]. Available: <http://bae.okstate.edu/faculty-sites/Darcy/DarcyWeisbach/Darcy-WeisbachEq.htm>.
- [22] G. O. Brown, 'The History of the Darcy-Weisbach Equation for Pipe Flow Resistance', in *Environmental and Water Resources History*, Washington, D.C., United States, 2002, pp. 34–43.
- [23] D. Citrini and G. Nosedà, *Idraulica*. Milano: Casa Editrice Ambrosiana, 1994.
- [24] B. E. Larock, R. W. Jeppson, and G. Z. Watters, *Hydraulics of pipeline systems*. Boca Raton, FL: CRC Press, 2000.
- [25] W. C. Walton, 'Selected Analytical Methods for Well and Aquifer Evaluation', p. 91.
- [26] 'Theis Solution for Nonleaky Confined Aquifers'. [Online]. Available: <http://www.aqtesolv.com/theis.htm>. [Accessed: 08-Jul-2019].
- [27] M. Abramowitz and I. Stegun, 'Handbook of mathematical functions'. 1968.
- [28] 'Cooper-Jacob (1946) Solution for Pumping Tests in Confined Aquifers'. [Online]. Available: <http://www.aqtesolv.com/cooper-jacob.htm>. [Accessed: 15-Jul-2019].
- [29] P. I. Polubarinova-Koch, *Theory of ground water movement*. Place of publication not identified: Princeton University Press, 2015.